Chapter 11

Wind tunnels for automobile aerodynamics

Wolf-Heinrich Hucho

11.1 Introduction

11.1.1 Requirements for a vehicle wind tunnel

Much development work is required to achieve the aerodynamic qualities and thermal characteristics of vehicles, as described in the previous chapters. In this work, the road is an important test instrument and in the final analysis this is where the results must prove themselves. The wind tunnel is however an essential development tool, with which reality is simulated—but not duplicated. Before attempting simulation of this type it is necessary to analyse the original phenomenon.

Figure 11.1[11.1] shows variables for air flow and thermal load. The air flow is composed of two fields, one resulting from the forward motion of the vehicle, the other from the natural wind (see Fig. 4.2). As indicated in Fig. 11.1 this natural wind field is similar to a boundary layer and causes a

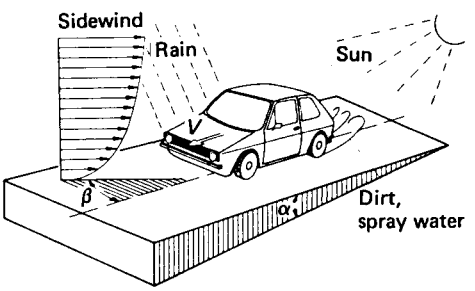

Figure 11.1 The vehicle in its true environment

twisted oncoming flow profile to develop (see Fig. 5.3). Gusts continuously change the wind speed and angle β of oncoming flow. The ground boundary layer of the wind is turbulent; the dimensions of the turbulence eddies are of the same magnitude as the length of the vehicle. For an observer moving with the vehicle, the gustiness appears to be increased by the fact that the vehicle drives through wakes resulting from bridges, houses, trees, etc. and through the flow field of vehicles driving in front and in the opposite direction. The flow field approaching the vehicle is therefore largely inhomogeneous and non-stationary and is considerably

more complex than that of an aircraft flying at high altitude. The requirements for the flow quality of an automobile wind tunnel therefore cannot be borrowed uncritically from aeronautics.

The temperature field above the road is also not always homogeneous. Intensive sunlight will heat the roadway more than the surrounding air so that a temperature boundary layer forms above the road.

The flow and temperature fields on the road can be simulated in a wind tunnel only in a highly idealized form; homogeneous fields are used. However, it is worth considering, from time to time, the much more complex real-life situation during the evaluation of test results.

The performance specification of the air conditioner in a vehicle is highly dependent upon the radiation from the sun, including diffuse radiation. The former may be simulated in simplified form in the wind tunnel in terms of the spectrum and direction; the diffuse radiation is usually not considered.

Much development work is done to channel rain water and spray, and to prevent the deposition of dirt, or to limit it to areas where safety will not be affected (see section 6.4). The simulation of rain in the wind tunnel is in fact relatively simple, but flow simulation of the soiling process is imperfect—due particularly to the expense of reproducing wheel rotation in the wind tunnel.

With the exception of model testing, all the above-mentioned development work can be performed on the road. The disadvantage of using the road as a test instrument is that conditions are seldom repeatable. It is also extremely difficult to find roads with a given gradient long enough to achieve a state of equilibrium for thermal tests. On the other hand, the acquisition, storage and processing of data during a road test now presents less of a problem, due to advances in electronics.

11.1.2 Simulation of road driving

Motor vehicle aerodynamics can be subdivided into four categories, both in regard to its objectives and, as explained below, in regard to the requirements it places on simulation techniques. These are illustrated in Fig. 11.2 for passenger vehicles,[11.2] and in Fig. 11.3 for commercial vehicles.[11.3]

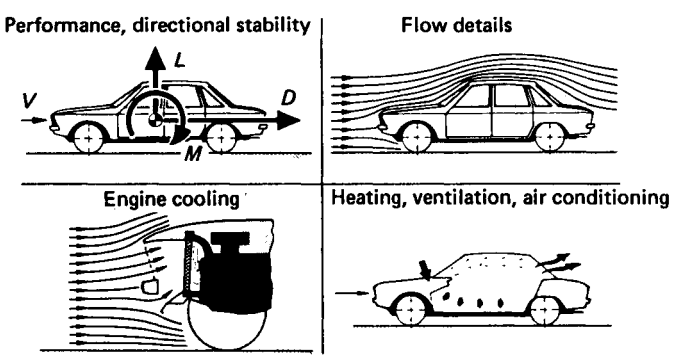

Figure 11.2 The main objectives of vehicle aerodynamics, passenger cars

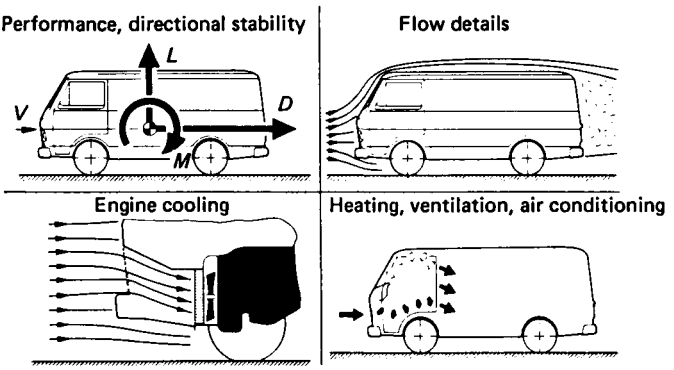

Figure 11.3 The main objectives of vehicle aerodynamics, commercial vehicles

For the *forces and moments* which determine driving performance and directional stability it is important to represent the actual air flow around the vehicle as closely as possible. Since the pressure p at every point (and therefore the effective forces and moments as integral variables) is proportional to the local flow speed v in the relationship

$$p \sim v^2$$

errors in the velocity distribution of the simulated flow field have a significant effect upon the test results. Within the limitations mentioned above—a homogeneous flow field—the air flow around the vehicle can be simulated quite well in a wind tunnel and close agreement between wind tunnel measurements and road tests has been achieved (see section 11.3).

In the wind tunnel the vehicle remains stationary and the wind blows by—the reverse of the situation on the road. Tests with towed vehicle models (common in naval architecture) are used when examining the non-stationary effects of side wind. (Section 5.2.3 describes some of the test equipment.) Towing systems are also used to simulate driving through tunnels (see section 8.5.5.2), and here there are parallels with railway

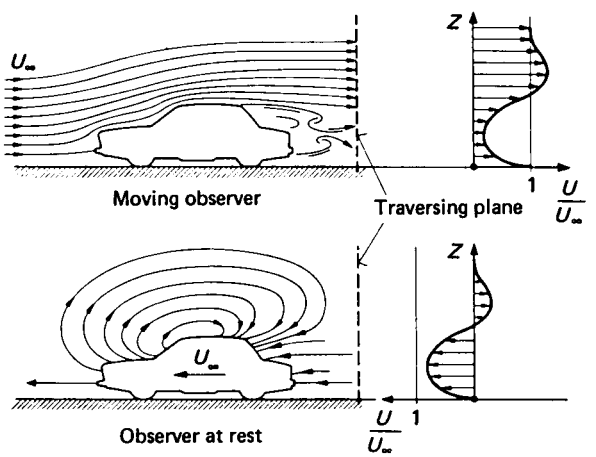

Figure 11.4 Change of the relative motion between road driving and wind tunnel testing

aerodynamics (see section 1.13). When performing wind tunnel tests, one must remain aware of the reversal of the motion sequence (Fig. 11.4).

The same requirements as regards forces and moments have to be placed on the quality of air flow around the vehicle when studying *flow details*. However, the wind tunnel alone is not sufficient for this purpose. For example, research on wind noise generation is limited by the high noise level in the wind tunnel. Also, tests on spray soiling must take into consideration the relative motion between vehicle and road and the rotation of the wheels, both of which present technical difficulties during wind tunnel tests.

Although less stringent requirements are placed on the quality of the air flow for development work on the *cooling system*, the tractive effort and the speed of the driving wheels as well as the air temperature must be simulated precisely. Air flow around the front of the car can be simulated relatively easily in combination with several correlation measurements. Special rigs are used for the development of cooling systems, which might be better described as 'climatic wind chambers' or 'chassis dynamometers with cooling air' rather than wind tunnels. Such systems are described in section 11.5.

For testing the *heater, ventilation and air conditioning*, simulation requirements are part way between those for purely aerodynamic tests and those for component cooling. The primary climatic parameters such as air temperature, humidity and solar radiation, as well as the influence of the engine, must be simulated precisely. The heat balance of the vehicle is highly dependent on the flow of air around and through it, so the convective heat flux, which is directly proportional to the quantity of air flowing through the passenger compartment, must also be simulated precisely. However, the heat flux $\dot{Q}_c$ resulting from conduction through the various parts of the body and heat transfer to its interior and exterior surfaces is

$$\dot{Q}_c \sim v^{0.5} \text{ to } v^{0.8}$$

The effect of an error in the local velocity of the simulated flow field is therefore less than proportionate. This is why 'climatic' wind tunnels with smaller jet dimensions and consequently greater velocity flow field deviations are acceptable.

As an alternative to simulating one main parameter and only approximating the others, all primary parameters may be simulated simultaneously and as closely as possible in a so-called 'large climatic wind tunnel'. Practical examples of all these possibilities are given in section 11.5.

Vehicle development work is usually shared among the above-mentioned test facilities. However, for this to be successful, precise information must be available on how the individual test results relate to driving on the road and how they can be compared with one another. In aeronautical research and ship testing much effort has been expended to discover and quantify the shortcomings of simulation by comparing wind tunnels, towing tanks, etc. using standardized calibration models. Corresponding research in automobile aerodynamics is described in sections 11.3.2 and 11.5.7.

11.2 Principles of wind tunnel technology

11.2.1 Recommended reading

Wind tunnel technology is dealt with in detail in standard works such as Pankhurst and Holder[11.4] and Pope.[11.5] Wuest[11.6] provides a short introduction to the most important details of wind tunnel technology. Details of recent research results, for example rational nozzle design or the execution of wind tunnel corrections (the so-called 'blockage corrections'), have to be sought in the journals; they have not yet been published in book form.

11.2.2 Design and function

The two types of wind tunnel are distinguished by the type of air guidance. In the Göttingen type tunnel with closed air return (Fig. 11.5, bottom) the fan drives the air in a closed circuit. The top illustration shows the Eiffel type tunnel, which takes in air from the surroundings and expels it to the

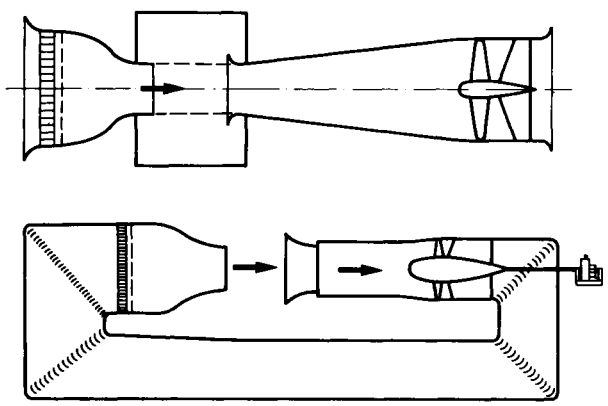

Figure 11.5 Wind tunnel with closed return (Göttingen type) and with open return (Eiffel type), after ref. 11.6

surroundings. In addition to these types there is a 'compromise' type with 'open return', often also connected with the name Eiffel. On this type the air from the outlet diffuser is returned to the inlet of the settling chamber upstream of the nozzle within a building surrounding the entire wind tunnel. In newer wind tunnels of this type the building is designed to return the air with the lowest possible losses. There are also some 'closed return' wind tunnels with two return ducts, but this approach can hardly be recommended. In addition to the higher cost of two return circuits and two drive units, they have the inherent problem of uncontrollable flow split and thus flow distribution in the test section. Examples of the first three types of construction are given in section 11.5. All types have intrinsic advantages and disadvantages, which can be compared quantitatively with one another only for a specific application.

The main advantage of the Göttingen type tunnel is its low power requirement, which reduces the operating cost due to the lower energy consumption itself as well as the lower electric power connection cost—a

considerable sum for larger wind tunnels. The cost of the drive unit (motor, fan, control) is lower, though that for the tunnel duct is considerably higher than for the pure Eiffel type. Most automobile models are made of plastilina, which loses its stability at higher temperatures. For this reason a cooler must be provided for the closed air return. The pressure loss resulting from the cooler requires additional power, thus some of the advantage of the lower drive power is lost. The closed return tunnel is the only type suitable for air-conditioning, and climatic work.

The Eiffel tunnel, set up outdoors, has a considerable disadvantage in that operation is dependent upon the weather; for this reason it is only practical in countries with moderate climates. Particular difficulties are presented in keeping the quality of the flow in the test section free from wind effects where the air is sucked in from outdoors. In the case of one large Eiffel tunnel in the automobile industry, it is known that on average one test day per week is lost due to unfavourable wind conditions. Screens in front of the intake nozzle, which also prevent leaves and birds etc. from being sucked in, eliminate the influence of the wind only when they are suitably designed. Their pressure loss has to be overcome by additional fan power. A further disadvantage of the outdoor Eiffel tunnel is its excessive noise.

However, the primary advantage of the Eiffel tunnel is its economical construction. If it exhausts outdoors, an exhaust gas extractor is not required for tests with the vehicle engine running. It is simple to construct an Eiffel tunnel with a test section closed on all sides, although an open test section is possible at slightly higher construction cost.

11.2.3 Construction elements

The size, performance and quality of a wind tunnel are mainly determined by the following elements:

- test section
- nozzle and settling chamber
- fan and drive.

In climatic wind tunnels a fourth significant construction element, the cooler, is added. Only these four elements are considered here; the reader is referred to the literature for details such as diffuser, deflection baffles, screens and flow straighteners, etc.[11.4,11.5]

The overall size of a wind tunnel is determined, above all, by the dimensions of the test section. The governing parameter is the cross-section A_T of the wind tunnel's nozzle. The ratio of the frontal area A of the vehicle to the cross-sectional area A_T of the wind tunnel air stream, also called the blockage ratio φ, should be as small as possible. On the road the blockage ratio is zero. If the frontal area for a car is assumed to be $2.0\,m^2$ (see Fig. 1.48), and if, as in aircraft aerodynamics, the blockage ratio should not exceed 0.05, a nozzle exit cross-section of $A_T = 40\,m^2$ is required. Of all automobile wind tunnels this requirement is fulfilled only by the wind tunnel at General Motors ($A_T = 65.9\,m^2$). None of the other wind tunnels used in automobile engineering meets this requirement, with the only exception of the Deutsch Niederländischer Windkanal (DNW),

which was designed for aeronautical purposes and is now also used for automobile testing. Comparative measurements between wind tunnels of different sizes (see section 11.5.7) indicate however that a considerably higher blockage ratio is permissible for automobile aerodynamics.

For economic reasons attempts are to be made to construct wind tunnels as small as possible. Two approaches are used, often simultaneously. In the first, attempts are made to simulate the flow in the open air by suitable shaping of the air stream boundaries of the smaller test section; in the second, the limits of the air stream dimensions are taken into consideration by applying empirical corrections to the measurement results. These corrections are described in section 11.3.3.

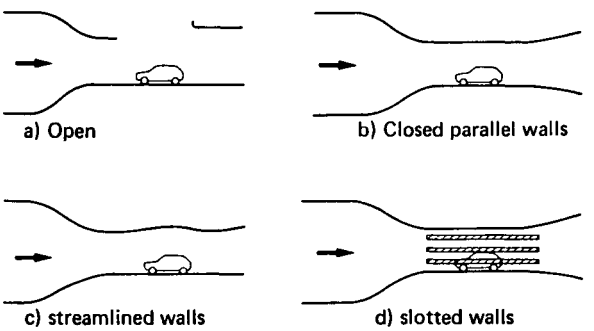

Figure 11.6 Classification of test sections according to the type of test section boundaries

In Fig. 11.6 four test sections are compared according to the type of the jet boundary; they all have a level floor, which represents the road. (The questions in relation to simulation of the road are discussed in section 11.3.2.) In the free jet ('open') test section, Fig. 11.6a, the air stream has three free boundaries, at which the air from the test stream mixes with the quiescent surrounding air as a free jet. This mixing leads to dissipation of the jet's core, that portion of the stream which contains the desired oncoming flow velocity V. This mixing limits the usable length of the test section.

The great advantage of the open test section is that, with a correctly matched collecting cone, the gradient of the static pressure along the axis of the tunnel is negligible. When measuring the drag of long bodies with large vertical surfaces at the front and rear, even small axial pressure gradients can lead to notable errors (buoyancy effect). Another considerable advantage is the lower absolute value of the blockage correction in comparison to closed parallel test sections. Finally, the accessibility of the open test section facilitates experimenting with and photographing the flow. Disadvantages are the higher loss coefficient of the free jet and the unimpeded sound radiation. For climatic tunnels with free jet test section, the chamber surrounding the test section must be included in the air-conditioned area.

The advantage of a closed test section, Fig. 11.6b, is its large usable length; the core of the air stream is dissipated much more slowly along a closed duct than in an open jet. However, the friction loss along the walls results in a pressure decrease along the axis of the stream. This pressure

decrease must be compensated for by slightly widening the tunnel cross-section in the flow direction. However, this compensation is only correct for one configuration, for example in the case of an empty test section; in all other cases it is only an approximation and where necessary must be further corrected through computation.

One disadvantage of the closed test section is its sensitivity to blockage; the absolute blockage correction value is approximately double that of a free jet. At a higher angle of yaw β, separation may result along the walls of the wind tunnel due to the high degree of deformation of the air stream; a correction for the angle of yaw is then no longer possible.

One way of overcoming the large blockage correction for the closed test section is to streamline the test section walls. In this case it is assumed that the flow pattern at a certain distance from the vehicle, the so-called far field, is no longer highly dependent upon the individual details of its shape. The far field is determined mainly by the primary parameters length, height and width (and thus the fineness ratio which can be derived from these).

There is little variation in the principal dimensions for passenger cars. The frontal area of an average family car is approximately 1.85 m^2, and the deviation between large and small cars is no more than ± 15 per cent, if we neglect subminiature cars. If the tunnel walls are shaped according to the flow pattern of an average car in the open air, the flow around smaller and larger vehicles will only be slightly distorted.

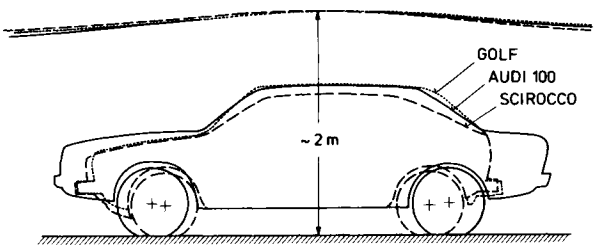

Figure 11.7 Comparison of the far flow fields of different passenger cars, using a selected streamline in the longitudinal midsection

A comparison of flow patterns using smoke to show the streamlines confirms this concept. As shown in Fig. 11.7, the flow pattern for various vehicles is very similar even at a height of only approximately 2 m above the roadway. Stafford[11.8] was able to show that with streamlined walls the same result could be obtained with blockage of 20 per cent as in a test section with parallel walls with blockage of only 5 per cent. Streamlined test sections are particularly recommended for climatic chambers with wind with a nozzle area of $A_T \approx 10\,m^2$. This is because it is not desirable to attempt a subsequent correction for an imperfect pressure distribution in this case, but rather to have a flow state during the test that corresponds to the climatic load on the vehicle while driving on the road.

Instead of having streamlined tunnel walls with a fixed contour the tunnel walls can be designed to be adaptive. A related concept has been developed by Whitfield et al.[11.9] In an iterative process, using a potential flow model for the far field ('exterior flow field'), the tunnel walls are

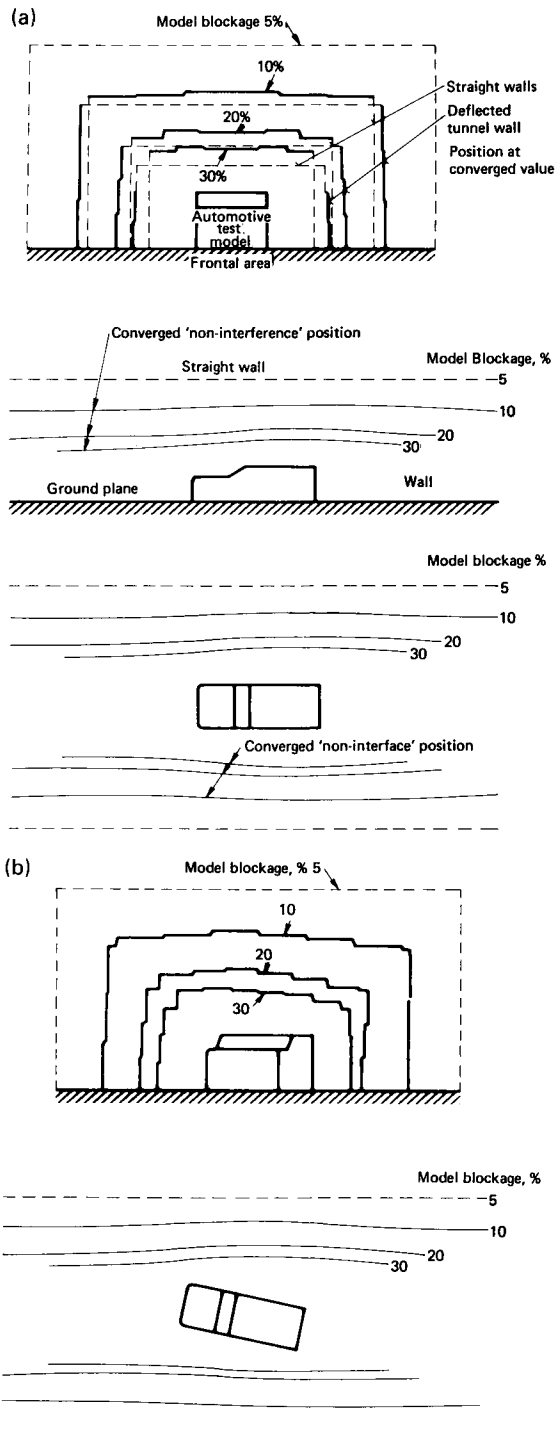

Figure 11.8 Adaptive tunnel walls at converged value for blockage ratios of 10, 20 and 30 per cent: (a) zero yaw; (b) yaw angle $\beta = 10°$; after ref. 11.9

streamlined such that flow angularity at the walls is the same as for the related streamline in an infinite flow field. According to ref. 11.9 this procedure will compensate in 8 to 10 iteration steps for blockage ratios up to 30 per cent, even for a yaw angle of 10°. Figure 11.8a, from ref. 11.9, shows the contours of the tunnel walls at converged value for blockage ratios of 10, 20 and 30 per cent for zero yaw, Fig. 11.8b for 10° yaw.

The slotted wall test section, Fig. 11.6d, is an attempt to combine the advantages of the open and closed test sections, and eliminate the disadvantages of both. This idea is attributed to Vandrey and Wieghardt.[11.10,11.11] Slotted walls are used in water tunnels and wind tunnels in marine hydrodynamics, to allow research on particularly long bodies with a sufficiently large Reynolds number. The automobile wind tunnels at the Institute Aérotechnique in St. Cyr, France (see Peters[11.12]), and at the Bayerische Motorenwerke AG (BMW) in Munich, Germany, also have test sections with slotted walls. The wind tunnels opened in 1986 by Volvo AB, Göteborg, Sweden, and Dr.-Ing. F. Porsche AG, Weissach, Germany, are also equipped with slotted walls. The open area ratio (free surface to covered surface) must be matched with calibration tests so that the pressure distribution corresponds closely to that in the open air. In the St. Cyr tunnel, an open area ratio of 28 per cent was established; see ref. 11.12. Flay et al.[11.13] found an open area ratio of 30 per cent to be an optimum for a blockage ratio of 14 per cent up to a yaw angle of 30°. This is confirmed by systematic measurements carried out by Waudby-Smith and Rainbird.[11.65]

The contraction ratio and contours of the wind tunnel nozzle have a decisive effect upon the quality of the air stream and the required fan power. The contraction ratio K (Fig. 11.9) is the area ratio of the nozzle

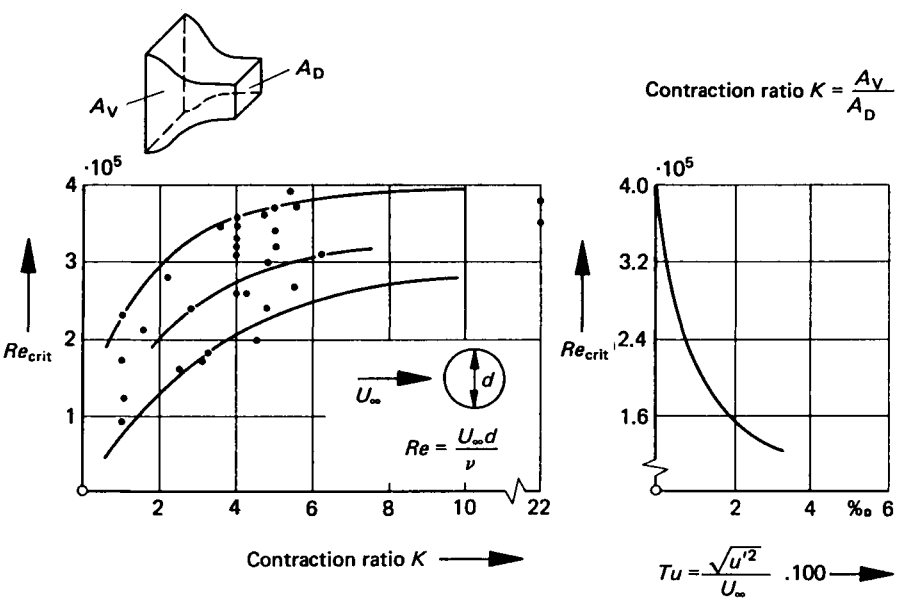

Figure 11.9 Critical Reynolds number and turbulence level of existing wind tunnel nozzles, after ref. 11.7

inlet to the nozzle outlet, $K = A_S/A_T$. Assuming a suitable nozzle contour, a larger contraction ratio provides a more uniform velocity distribution over the air stream cross-section and a lower turbulence level. In order to achieve these objectives, wind tunnels for aircraft aerodynamics are designed with a large contraction ratio (Bradshaw and Pankhurst[11.14] recommend $K = 10$ to 12). Automobile wind tunnels usually have a smaller contraction ratio: $K = 4$. For Eiffel type wind tunnels, a considerably smaller contraction ratio is sufficient; $K = 2$ to 3 is often selected.

The tendency towards larger contraction ratios in vehicle work is more attributable to the attempt to minimize the power requirement. If a fan drive power of P_0 corresponding to a contraction ratio of K_0 is assumed, the decreasing power requirement with increasing contraction ratio shown in Fig. 11.10 results, according to an estimate made by Piatek.[11.15] Here it is assumed that the jet power remains constant. Therefore, to a first approximation, the losses in the nozzle, test section and collecting cone remain the same while the losses in the remaining parts of the wind tunnel decrease when the geometric similarity is maintained at $(1/K_{new} : K_0)^2$. The maintenance of the geometric similarity naturally results in an increasing volume for the tunnel for increasing contraction ratios. If the short diffuser recommended in ref. 11.14 is attached in front of the settling chamber the construction volume can be reduced, but the reduction of the required drive power is then not as great as shown in Fig. 11.10.

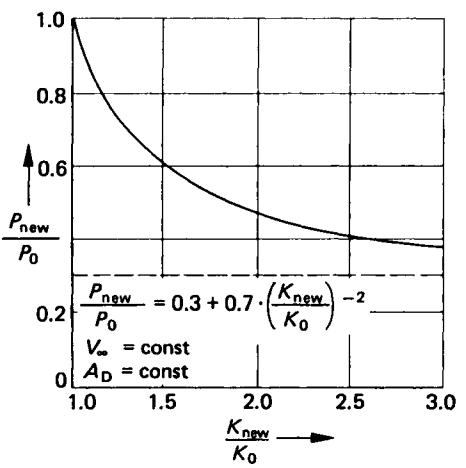

Figure 11.10 Reduction of required fan power for a wind tunnel with increasing contraction ratio K of the nozzle. In wind tunnels with coolers approx. 30 per cent of the total losses are generated in the nozzle, the test section and the collecting cone. Jet power remains constant; after ref. 11.15

In addition to the contraction ratio, the contour of the nozzle also determines the quality of the wind tunnel flow field. The velocity should be uniform at the nozzle exit yet for reasons of cost the nozzle should be as short as possible. The local velocity vector should also be as near parallel as possible to the axis of the tunnel. Of the numerous recommendations for calculation of the nozzles to date, that proposed by Witoszynski[11.16] was preferred, though it applies only to axially symmetrical flow and does not

provide any information on the selection of nozzle length. Good results have been achieved with nozzles whose length corresponds approximately to the inlet diameter, particularly when the recommendation of Prandtl is followed and the nozzle is widened slightly at the outlet. Recently published numerical procedures have been based upon the principle of iterative computation of the potential flow and the boundary layer: a contour is prescribed and then varied until the desired uniform velocity distribution results at the nozzle outlet. A procedure of this type was presented by Börger[11.17] for two-dimensional and axially symmetrical flow; the formation of the boundary layer is also taken into consideration in the computation of the contour. Figure 11.11 shows the contour computed by

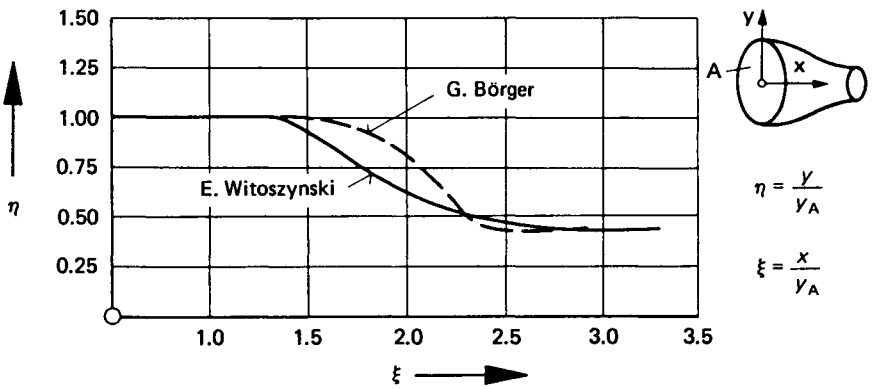

Figure 11.11 Comparison of nozzle contours according to Witoszynski and Börger, axial symmetry, after ref. 11.17

Börger compared with that according to Witoszynski; the slight widening of the contour at the outlet is a result of the computation from Börger. Börger designs the nozzle shorter than Witoszynski with better (computed) velocity distribution at the outlet. No experimental confirmation of these results has yet been published to the knowledge of the author.

A procedure for designing axially symmetrical nozzles by Morel[11.18] leads to contours very similar to those of Börger. The nozzle design is accomplished on the basis of draft diagrams; but again experimental confirmation is lacking.

The air stream velocity in the wind tunnel must be continuously controllable. In automobile work precise tests at very low wind speed are important. As explained in Chapter 9, driving slowly up a long steep gradient represents a critical case for the dimensioning of the radiator. In such cases the relative wind as well as the radiator fan contribute to the cooling effect; precise control of the relative wind is essential.

Two basic solutions are available for control of the wind velocity: variable-pitch blades at constant fan speed or variation of fan speed with fixed blade angle. Variable pitch has the advantage that the velocities can be changed very quickly and the drive is simple. The disadvantage is the high noise level at all wind speeds, even at zero wind speed. With the use of pole-changing asynchronous motors, a second lower fan speed is possible for wind noise tests. Further disadvantages of blade pitch control are the

mechanical complexity and sensitivity of the blade pitch-changing mechanism as well as the high inertia of the rotor. The latter disadvantage has now been overcome by the use of light-weight technology from aircraft construction.

Fan speed control is used for newer wind tunnels. The fan blades are of light construction; wood or fibre-glass laminates are used. Thyristor controls have generally replaced the Ward-Leonard system. The possibility of driving the fan directly with a heat engine, such as a propeller turbine, has yet to be explored.

The layout of the wind tunnel cooler must accommodate other aspects than steady-state operation. It is important that the cooler performance is sufficient to allow the desired temperature to be reached quickly. In order to keep the pressure loss through the cooler as small as possible, it should be installed at a point with a large cross-section. A position at the end of the large diffuser downstream of the fan appears to be more suitable than a location inside the settling chamber (see also section 11.3.1).

11.2.4 Equipment

A six-component balance is required for force measurements (see section 12.1.1). In full-scale automotive wind tunnels, balances mounted underneath the test section are preferred.

In addition to the simple model assembly, these balances offer the great advantage that no corrections are necessary for suspension wires or struts. It is only necessary to correct for the lift on the wheel support plates. This takes into consideration the fact that, as a result of the displacement flow around the wheel, a low pressure field is formed on the plate, which results in lift acting upon the plate surface not covered by the wheel.

The traditional beam and lever balances with moving balance weights are being replaced by balances with load cells in combination with preload weights.

The test equipment in an automotive wind tunnel also includes high-performance pressure and temperature measuring instruments. In view of the pressures of time and cost an on-line, real-time process computer is nowadays considered essential.

Other typical features of motor vehicle wind tunnels are an engine cooling water simulation unit, to allow development of the radiator even during the model phase, as well as a device for measuring the volume of air passing through the passenger compartment (see section 12.1.5).

Climate simulation is required for thermal tests; air temperature, solar radiation and relative humidity to tropical rain levels must all be simulated. During tests the propulsion system of the vehicle can be loaded with a chassis dynamometer, but the lost tractive force at the drums must be considered, and also the fact that the rolling resistance of the tyres on drums is different from that on a level road.

Good lighting is required for flow observation. Smoke or oil vapour can be made easily visible in a darkened room, under proper illumination. Wakes are generally illuminated over a large surface (see Fig. 1.2); for photographing flow patterns with individual smoke trails, a planar light source (or slit) is more suitable, as in Fig. 1.1 (see Hucho and Janssen,[11.19] and Takagi et al.[11.20]).

11.3 Limitations of simulation

11.3.1 Air flow quality

A uniform velocity distribution over the cross-section of the air stream is not only important for simulation but also to facilitate comparison between tunnels. With a contraction ratio of $K = 4$ and correct nozzle design, a velocity distribution can be achieved in which the local velocity does not deviate more than ± 1 per cent from the mean velocity except at the edge of the jet.[11.21] This is sufficient for automobile aerodynamics purposes.

It is important that the wind tunnel air stream be aligned precisely relative to the test vehicle. In automobile wind tunnels, the boundary layer which forms on the ground plane increases the effective angle of attack. As shown in Fig. 4.112, the angle of attack has a considerable influence upon the drag, particularly when edge radii are optimized using the procedure described in section 4.4.1. Asymmetries in the chamber surrounding the test section of an open-jet wind tunnel can produce an angle of yaw in the wind tunnel stream. As long as this remains small it has only a slight influence upon the drag (Fig. 4.115). However, a precisely directed jet is required for exact determination of the lateral forces and moment. Despite the extra cost it is best to make the wind tunnel nozzle adjustable so that the air stream can be set to the exact direction.

In climatic wind tunnels attention must be given to uniform temperature distribution over the cross-section of the air stream. Due to the cross-flow characteristics of the heat exchanger and the resulting non-uniformity in the temperature distribution it is worth installing the heat exchanger as far as possible upstream from the wind tunnel nozzle in order to allow any temperature non-uniformity to decay by mixing over a longer flow path.

11.3.2 Ground plane boundary layer

The relative motion between the road and vehicle is simulated only in exceptional cases. As a rule, the level floor of the test section is used as the

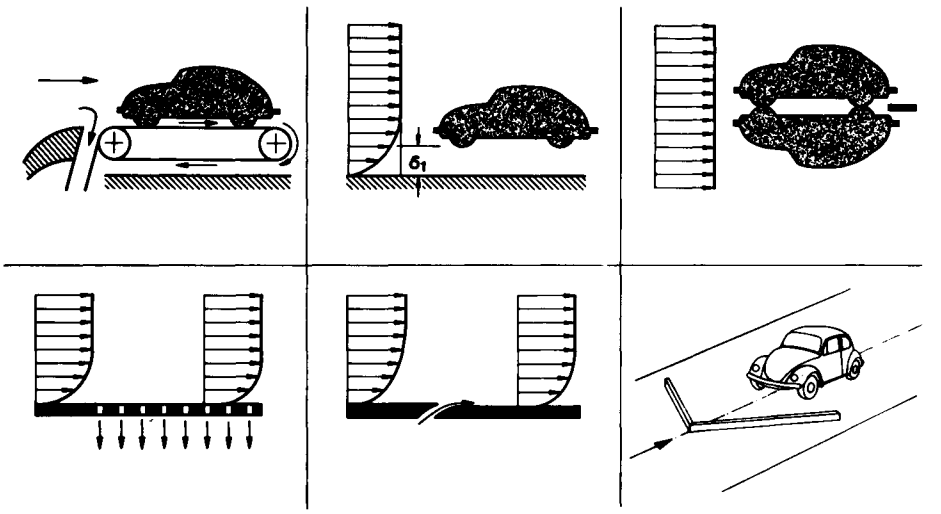

Figure 11.12 Possibilities for simulation of the road in the wind tunnel, after ref. 11.22

road. As a matter of principle the boundary layer that forms on the floor of the test section results in a different flow field than during driving on the road. A series of suggestions have been made to improve the simulation of the road in wind tunnels. These are summarized in Fig. 11.12 (from ref. 11.22).

One solution to this simulation task is the use of a running belt. As shown in Fig. 11.13, from ref. 11.23, the floor boundary layer can be virtually eliminated in this manner. This has also been confirmed with measurements performed by Rose and Carr.[11.24] However, the support of

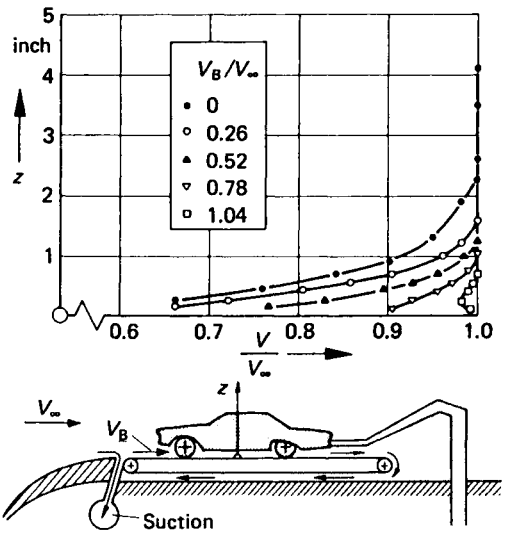

Figure 11.13 Simulation of the road with a moving belt, after ref. 11.23

the model over the moving belt presents difficulties, particularly with large and heavy models. Moreover, Beauvais et al.[11.23] have shown that the error in drag and particularly in lift, resulting from the flow in the gap between the wheels and belt, is greater than the influence of the ground boundary layer. Conversely, Ohtani et al.[11.25] state that lifting of the vehicle by the amount of the displacement thickness of the ground boundary layer has no effect upon the flow around the vehicle and the effective forces.

Potthoff suggested limiting the width of the running belt to the space between the wheels. The vehicle can then be supported with its tyres on the pads of the balance underneath the tunnel floor. However, no test results using this technique have yet been published.

The mirror image technique, which was preferred in the early days of automotive aerodynamics, is not practical. In addition to the difficulties listed in ref. 11.22 a second model and, if the blockage is not to be changed, a wind tunnel with double the nozzle cross-section are required.

Suction of the boundary layer is a practical method of reducing the boundary layer thickness. If accomplished as described in ref. 11.22, only suction through a slit or through a narrow strip of porous floor plate upstream of the model need be used.

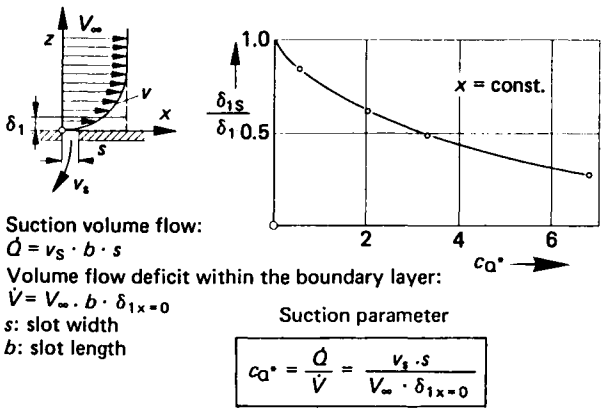

Figure 11.14 Reduction of the displacement thickness δ_1 of a turbulent boundary layer by slot suction, after ref. 11.22

Figure 11.14, from ref. 11.22, shows the relationship between the volume $\dot{Q}$ which is sucked off and the reduction of the displacement thickness δ_1 of the floor boundary layer for slot suction; this diagram is based on the tests performed by Arnold.[11.26] A slot suction system for the Volkswagen AG climatic wind tunnel was designed (but not installed) for the largest suction parameter considered here of $c_Q^* = 7$. The suction slot was to be positioned in front of the vehicle, and a reduction in the displacement thickness of 60 per cent was expected for the empty test section at the middle of the balance turntable (see Fig. 11.15). Approximately the same results were obtained with the boundary layer suction system in the Fiat wind tunnel in Turin by Antonucci, Ceronetti

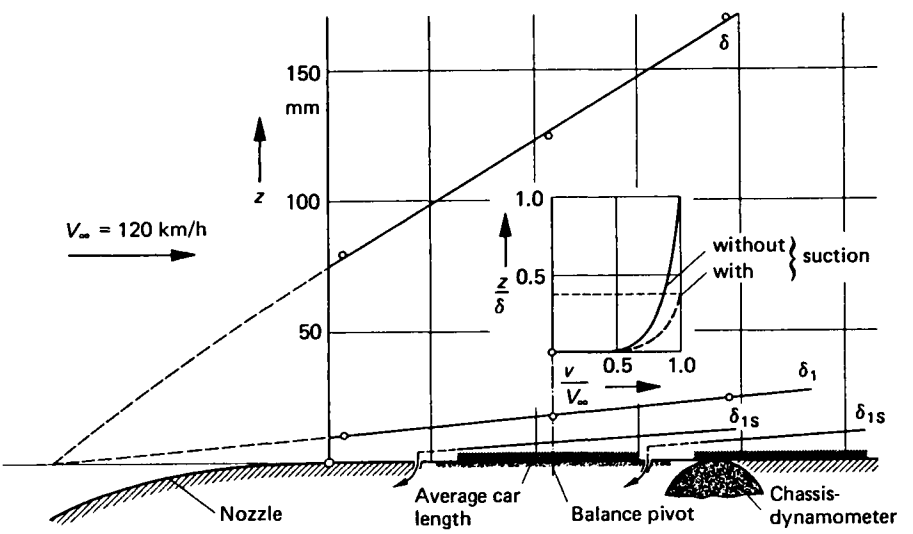

Figure 11.15 Possible reduction of the displacement thickness δ_1 of the floor boundary layer, Volkswagen climatic wind tunnel, by slot suction; suction parameter $c_Q^* = 7$; after ref. 11.22

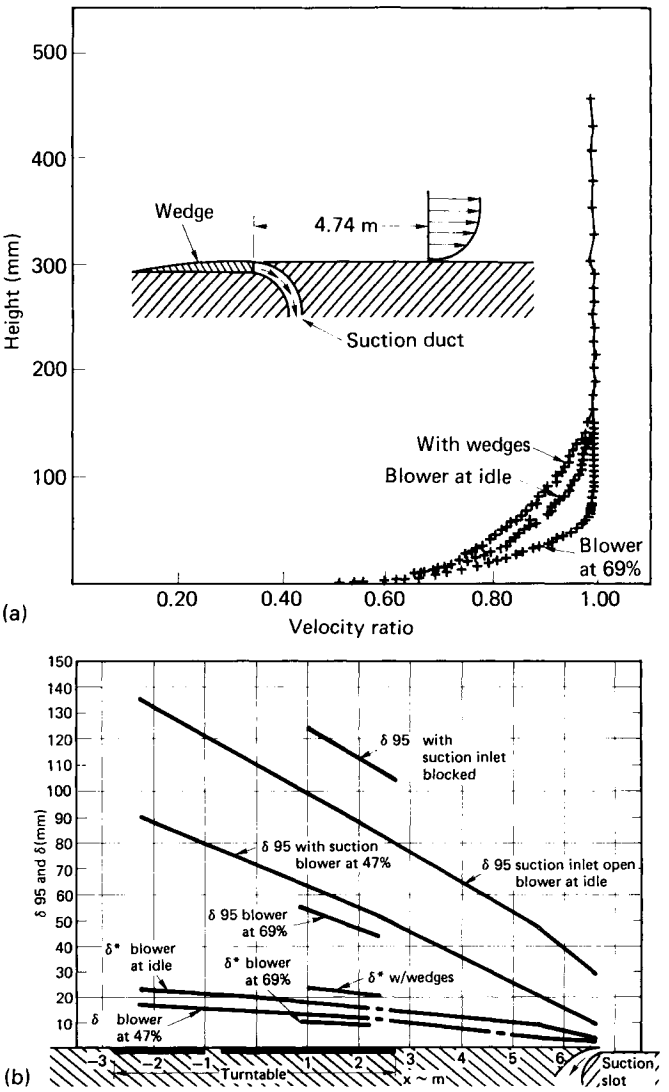

Figure 11.16 Test section floor boundary layer in the General Motors wind tunnel ESAL, after ref. 11.21: (a) velocity profiles without and with suction; (b) boundary layer growth at 80.5 km/h (50.3 mile/h)

and Costelli[11.27] and in the large wind tunnel of General Motors in Warren, Mich.; see Kelly, Provencher and Schenkel[11.21] (Fig. 11.16).

Blowing air into the retarded flow near the ground plane is another way of reducing the boundary layer thickness. Figure 11.17, from ref. 11.28, shows the blowing device used in the Lockheed Georgia wind tunnel. At about 2 m downstream from the row of nozzles the momentum loss of the boundary layer was almost completely compensated.

According to Gould[11.29] the boundary layer thickness can be reduced by one-half with trip mouldings placed on the floor in the form of an arrow

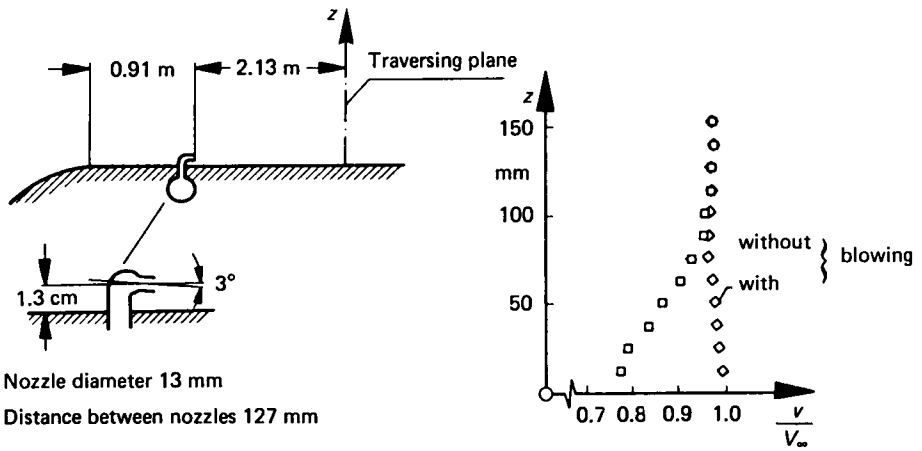

Figure 11.17 Reduction of boundary layer thickness by blowing air into the boundary layer, after ref. 11.28

(see Fig. 11.12). However, as Carr and Hassel[11.30] established, this measure has no notable effect upon the forces and moments acting upon vehicles with normal ground clearance.

Comparative measurements between wind tunnel and road performed by Hucho, Janssen and Schwarz[11.22] (Fig. 11.18) show that the velocity profile underneath the vehicle is only influenced by the ground plane boundary layer of the wind tunnel in the immediate vicinity of the test section floor. The displacement flow around the vehicle completely changes the velocity distribution in the channel formed by the vehicle's underside and the floor of the test section in comparison to that with an

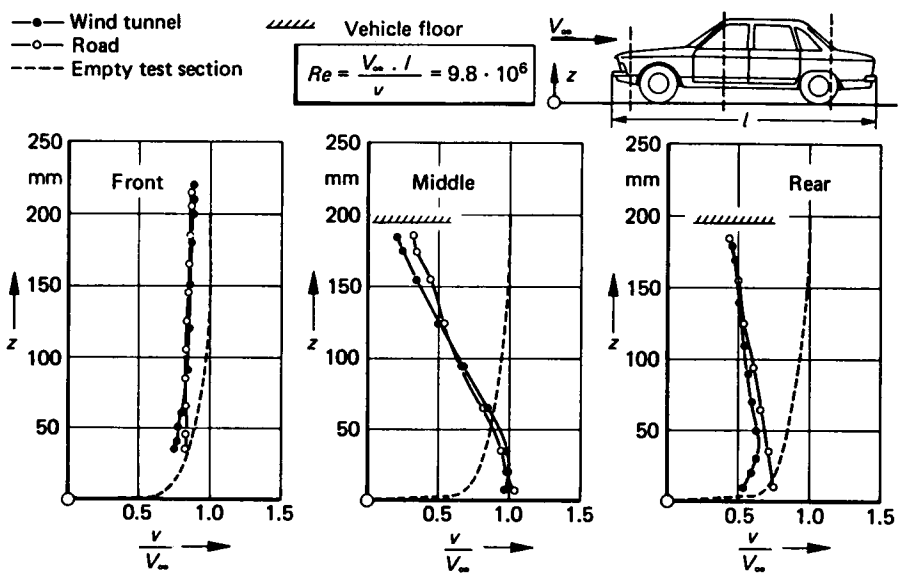

Figure 11.18 Velocity profiles beneath a car, wind tunnel versus road; after ref. 11.22

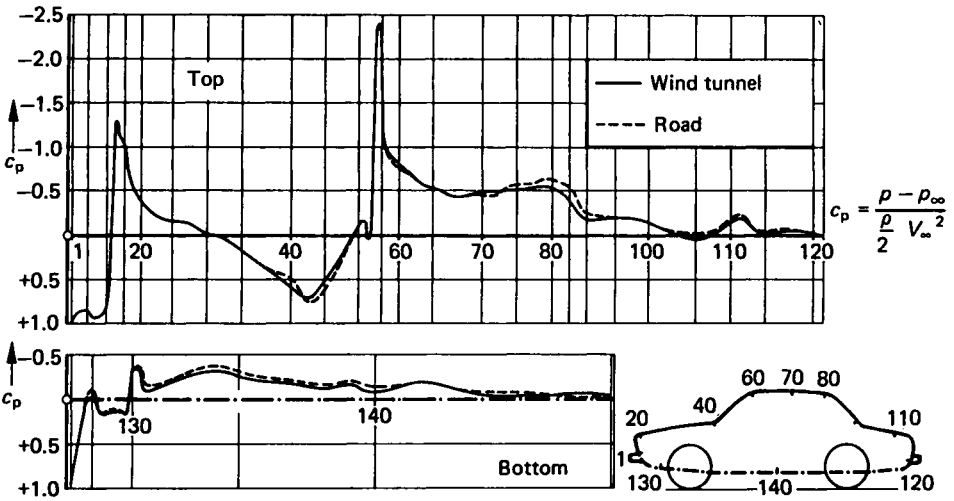

Figure 11.19 Pressure distribution along the longitudinal midsection of a passenger car, wind tunnel versus road; after ref. 11.22

empty test section; a comparatively thin boundary layer forms. As shown in Fig. 11.19 there is very good agreement between wind tunnel and road results for pressure distribution. This shows that the forces and moments measured in the wind tunnel are the same as those on the road if the prerequisite stated in ref. 11.22 is fulfilled, i.e. the ratio of the displacement thickness δ_1 to the ground clearance e of the vehicle is at least

$$\frac{\delta_1}{e} \leqslant 0.1$$

Other measurements given in ref. 11.22 on a sports car (less ground clearance) show that there is no significant boundary layer influence even for values of $\delta_1/e \approx 0.05$ (see also section 11.5.7). Thus, for passenger cars and vans, the need to improve road simulation by control of the boundary layer of the wind tunnel floor is eliminated. For vehicles with very low ground clearance, such as racing cars, the influence of the boundary layer has not yet been examined but a higher influence can be expected. The method suggested by Williams[11.28] of re-energizing the boundary layer by blowing in air appears to be particularly well suited for this type of application.

11.3.3 Air flow blockage, streamline deformation, pressure gradient

The flow of air around a vehicle in the wind tunnel is influenced by the flow conditions existing at the boundaries of the jet. The closer these boundaries are to the model the more the flow around the model is changed, compared to an infinitely large jet cross-section. In a closed test section the streamlines around the vehicle are forced closer together, in an open test section they widen out (see Fig. 11.20 from Wuest[11.6]). In the first case, the effective approach velocity is greater, in the second less than

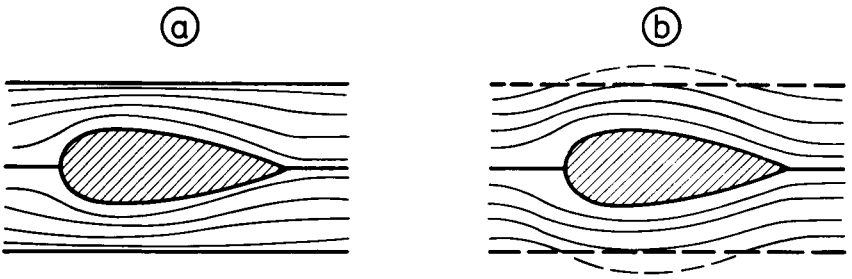

Figure 11.20 Effect of the flow boundary on the flow field, after ref. 11.6: (a) narrowing in a closed test section; (b) widening in an open test section

that at the nozzle. Without correction, this leads to drag coefficients which are too large in a closed test section and too small in an open test section. The same applies for all of the other force and moment coefficients.

Through corrections an attempt is made to take the finite character of the air stream dimensions into consideration and to convert the measured data to road conditions. In ref. 11.6, Wuest summarized how these corrections can be performed in aircraft aerodynamics. The correction formula for the drag contains the blockage ratio φ (they are therefore designated blockage corrections) and the drag of the test body as the primary variables. The corrections are only applicable when their magnitude is small, i.e. with small blockage and low drag figures. However caution is required in applying aircraft correction formulae to motor vehicle aerodynamics. In comparison to aircraft, motor vehicles are bluff bodies with high drag and large zones of flow separation, particularly in the wake. Motor vehicles therefore 'disturb' the wind tunnel stream much more than aircraft at the same geometric blockage ratio. Carr[11.31] attempted to take this into consideration by working out empirical correction formulae for motor vehicles. A recent survey on wind tunnel blockage corrections has been presented by Buchheim et al.[11.32] The corrections have been derived from comparative measurements among major European and North American automotive wind tunnels. A generally valid solution for the blockage correction for measurements on motor vehicles has not yet been found.

Wuest[11.6] showed that, for a wind tunnel whose jet has three free boundaries and one rigid boundary—the tunnel floor—the value of the blockage correction is small. For a large full-scale wind tunnel (see section 11.5) correction factors of maximum 2 per cent result for passenger cars. As the blockage correction itself is unreliable, this correction is generally neglected for large free jet wind tunnels. In contrast, closed test sections need relatively high correction factors. Moreover, these have the opposite sign, which must be taken into consideration when comparing measured results from wind tunnels with open and closed test sections.

When performing thermal tests, for which the effective wind speed must usually be equal to the circumferential speed on the drums of the chassis dynamometer, other procedures must be used for the application of correction factors than for aerodynamic tests. Here the measured data cannot be corrected after completion of the test according to correction

formulae; the corrected wind speed must prevail during the test. As a rule, the reference velocity is selected or adjusted for which the pressure coefficient at the stagnation point is $c_p = 1$ (see section 2.3.2 and Iwase, Yamada and Koga[11.33]).

If the vehicle is yawed to the oncoming flow the wind tunnel flow is deflected. In an open test section the jet can deflect laterally. The high curvature of the flow lines compared with those in the open air influences the field upstream of the vehicle. The effective angle of yaw is therefore smaller than the geometric angle of the vehicle relative to the axis of the working section.

In a closed test section the relationships are reversed. At large angles of yaw there is also the danger that the flow will separate from the test section walls.

Since the lateral force created by the wind passing a yawed car is equivalent to the lift on an aerofoil of low aspect ratio at an angle of attack (see Hucho and Emmelmann[11.34]), the correction mode for angle of attack could be used to correct for yaw angle in vehicle measurements, but in practice no yaw correction is applied. This is justified as long as the further processing of the vehicle aerodynamic derivatives is associated with further and very much greater uncertainties, such as the mechanical models used and the characteristics of tyres and other components.

The effect on vehicle drag of a pressure gradient along the axis of the air stream has already been discussed in section 11.2.3. A 'buoyancy' correction based on the pressure gradient in the empty test section must be considered questionable.

11.4 Tests with scale models

11.4.1 Model techniques

Even today, many tests are still performed on scale models. These tests are comparatively inexpensive; a further advantage is the handiness of smaller models for transport and for shape modifications. The most common scale in Europe for passenger cars is 1:4, though in small model tunnels 1:5 is also used. In the USA the '3/8 scale' is most common. For commercial vehicles a scale of 1:10 is popular. If a large wind tunnel is available, 1:2.5 is selected, see section 8.5.2.

However, in the development of passenger cars the use of reduced scale models is decreasing because the transferability of model tests to full-scale is uncertain; this is discussed in greater detail in the next section. Also designers prefer working on full-size models; judging the shape of scale models is very difficult. Details in the shape such as indentations, curvatures, window recesses, tyre beads and welts are overemphasized as a rule on scale models. On full-scale models, which represent the basis for model selection and later design, these exaggerations are reduced. Therefore one of the basic prerequisites for performing tests on scale models, the geometrical similarity to the full-scale version, is not fulfilled. However, if the wind tunnel model is produced by reducing the size of an existing full-scale model this problem is eliminated. A scale of 1:4 is then just large enough to reproduce all of the primary details to scale.

Since the underside of the vehicle has a great influence upon the flow of air around the vehicle (see section 4.3.2.7) all of its significant parts must also be represented.

Full-size models are generally built on an existing (reinforced) chassis; in this manner the flow of cooling air through the vehicle can also be simulated, an absolutely necessary prerequisite for optimization of the front of the vehicle.

Since the vehicle position has an influence upon the flow of air around the vehicle, it must be fixed precisely and adjusted for reproducibility. There are two possibilities for testing a vehicle in the ready-to-drive state: either the suspension is fixed in a given position, or the suspension remains free. In the latter case the vehicle is loaded with one half of the maximum permissible load so that it is in the design position. According to the aerodynamic forces and moments, the vehicle will adopt a similar attitude in the tunnel as when driving on the road. However, as a rule the suspension is fixed for tests on full-scale models. Models are considerably heavier than the finished vehicle, so that the effect of the air forces and moments on the vehicle position would be unrealistic.

The rotation of the wheels is usually not taken into consideration in wind tunnel testing; testing is carried out with the wheels stationary. When the wheels are integrated into the body the rotation of the wheels appears to have a negligible influence upon the forces and moments acting upon the vehicle. For soiling tests the 'spray pattern' of the rotating wheel can be reproduced by blowing in water drops or talcum (to simulate dust) at the appropriate points. When the wheels are not integrated into the body, as in single-seat racing cars, the forward displacement of the separation resulting from the rotation of the wheel can be taken into consideration by attaching a trip moulding (Williams,[11.35] see Fig. 11.21). The flow pattern is then very similar to that of a rolling wheel.

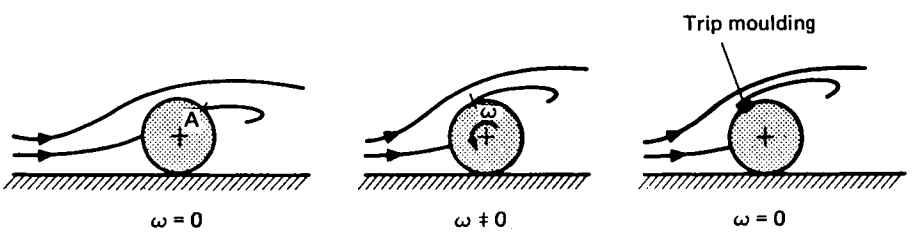

Figure 11.21 Simulation of the wheel rotation for a free rolling wheel by attachment of a trip moulding, after ref. 11.35

For force measurements on trucks with uncovered wheel sets, the rotation of the wheels is also neglected. Since the flow in the area of the chassis is largely separated, this should be permissible.

The simulation of the wheel and its rotary motion has been investigated by Cogotti.[11.36] His pressure measurements, reproduced in Fig. 11.22, clearly show the effects of ground clearance and wheel rotation. High negative pressures are induced on the tunnel floor and on the lower surface of the wheel as well, when the wheel is off the ground. These negative pressures increase sharply with decreasing ground clearance, causing

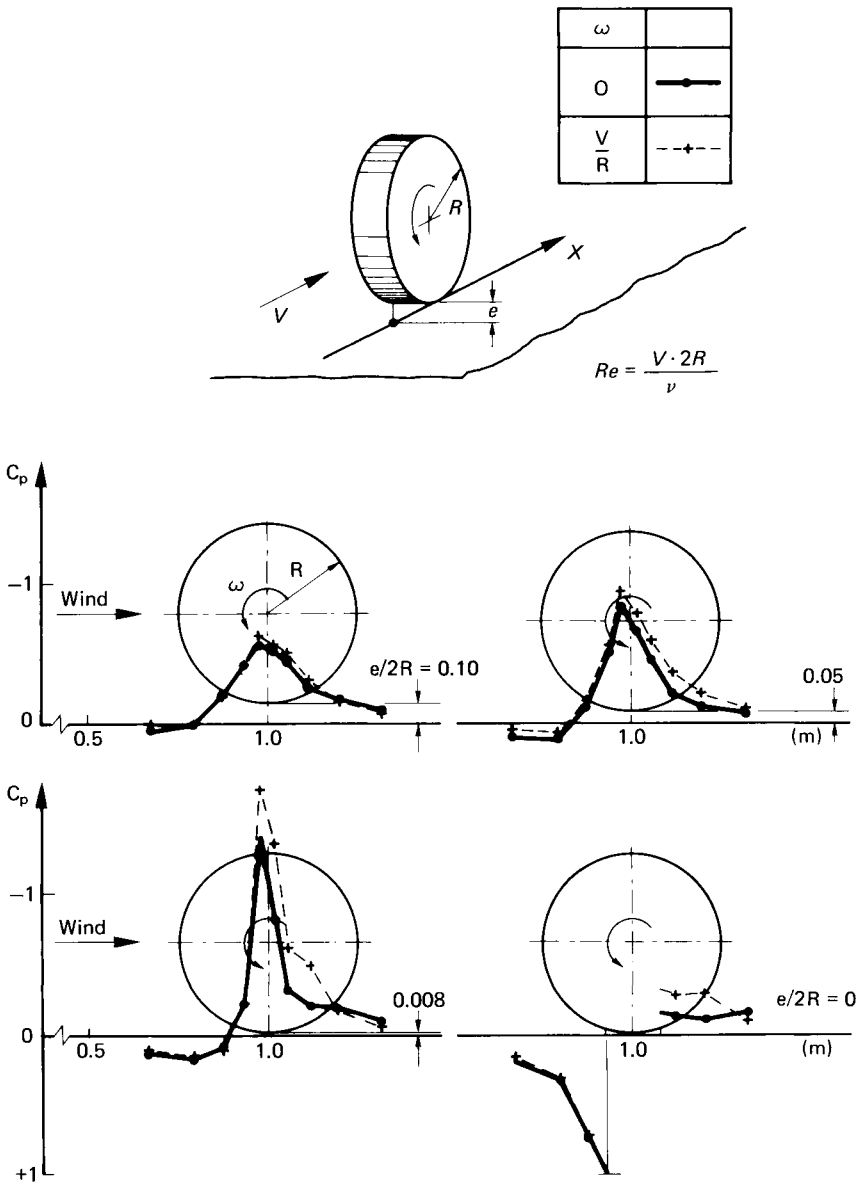

Figure 11.22 Pressure distribution on the floor beneath a wheel for different ground clearances, after ref. 11.36

negative lift. The effect of rotation on the pressure underneath the wheel is small. When the wheel just touches the ground, the pressure in front of the wheel is changed to a positive value, causing a significant change in lift from negative to positive, see Fig. 11.23. While the effect of rotation is small on drag, it is remarkable on lift. From Cogotti's experiments it can be concluded that for correct simulation of the flow around the wheel it is more important to maintain its contact to the ground than to reproduce its

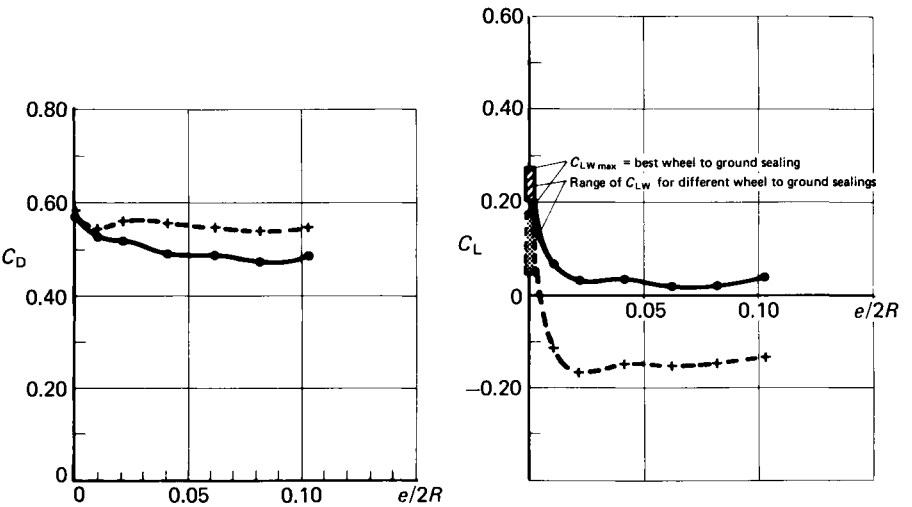

Figure 11.23 Drag and lift of a wheel, rotating and stationary, for different ground clearances; after ref. 11.36. —•— $\omega = 0$; – – + – – $\omega = V/R$

rotation. The drag of the non-rotating wheel is only slightly higher than that of the rotating wheel. But as soon as the wheel is shielded by a fairing, rotation starts to play an important role. Cogotti found that fairing a fixed wheel resulted in a drag reduction of $\Delta c_D = -0.049$, whereas this value

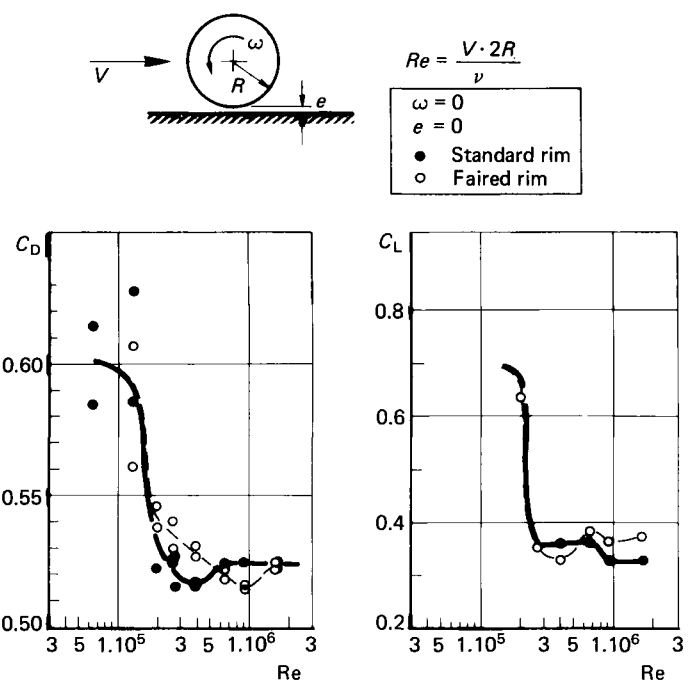

Figure 11.24 Drag and lift of a stationary wheel versus Reynolds number, after ref. 11.36

was $\Delta c_D = -0.091$ for the rotating wheel. The optimization of the flow around the wheel has to be done with the rotating wheel.

The Reynolds number has a significant influence on the flow around a wheel. This is to be seen from Fig. 11.24 for an isolated, stationary wheel. The plot of the drag coefficient c_D versus Reynolds number Re is similar to that for the circular cylinder. A drastic drag reduction occurs in the range of

$$10^5 < Re < 10^6$$

When small-scale models are tested, especially those with exposed wheels like single-seat racing cars, provision has to be made to be beyond the 'critical' wheel Reynolds number of 10^6.

11.4.2 Influence of the Reynolds number

In addition to the requirement for geometric similarity, the flow around the model and the full-scale version must be mechanically similar. For incompressible flow this condition is fulfilled when the Reynolds numbers for the scale model and full-scale version are equal, see Schlichting and Truckenbrodt[11.37] for example. The Reynolds number is defined as

$$Re = \frac{V_\infty l}{\nu}$$

see also section 2.2.1. V_∞ is the velocity of the undisturbed oncoming flow, l the length of the vehicle and ν the kinematic viscosity of the working fluid. Mechanical similarity is therefore present when the following equation is true:

$$\frac{V_1 l_1}{\nu_1} = \frac{V_2 l_2}{\nu_2}$$

Since, as a rule, model testing is accomplished in air (tests in water tunnels are seldom performed on vehicle models) the requirement for mechanical similarity is satisfied when the products of the velocities and lengths are equal. This condition is generally not maintained in tests on models with a scale of 1:4; the Reynolds numbers amount to one-quarter to one-half of the value of the full-scale version.

Since the drag resulting from friction is small in comparison to the drag resulting from pressure for motor vehicles (see section 4.3.1) it could be assumed that the influence of the Reynolds number is small within the stated Reynolds number range. In fact, drag measurements on vehicles exist that show hardly any Reynolds number influence. However, the following two examples show that serious errors can result through violation of the Reynolds law of similarity:

Figure 11.25 (after Hucho, Janssen and Emmelmann[11.38]) shows a series of measurements obtained during optimization of the front end of two vans. In both cases the objective was to find that radius between the front wall and side wall around which the air could just flow without separation, and which is therefore 'optimum' within the sense of the definition according to section 4.4.1. Van A had a relatively highly cambered front

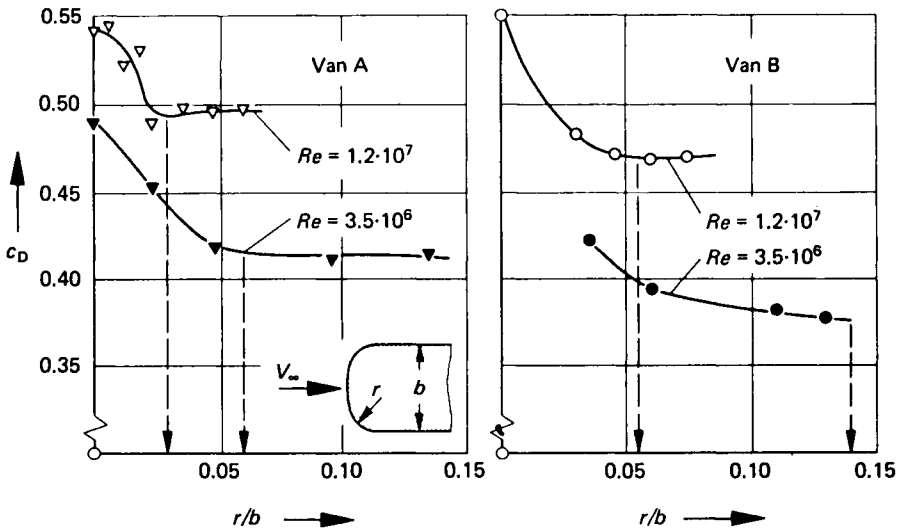

Figure 11.25 Influence of Reynolds number on 'optimum' radius at the transition from the front end to the sidewall of two different vans, after ref. 11.38

end; on the model with the scale of 1:4 the optimum radius in relation to the vehicle width was found to be $r/b = 0.06$. On van B, which was characterized by a very flat front end, the optimum radius on the 1:4 model was found to be $r/b \approx 0.14$. This radius was so large that it was rejected by the designers. The 'optimum' radii established for the models with a scale of 1:4 were checked on the full-scale versions. In both cases, optimum radii were found for the full scale versions that were considerably smaller than those found on the models. In the case of van B, the optimum radius for the full-scale version resulted in a stylistically acceptable solution.

The fact that air flows around considerably 'sharper' corners without separation on the large versions than is the case with small models is

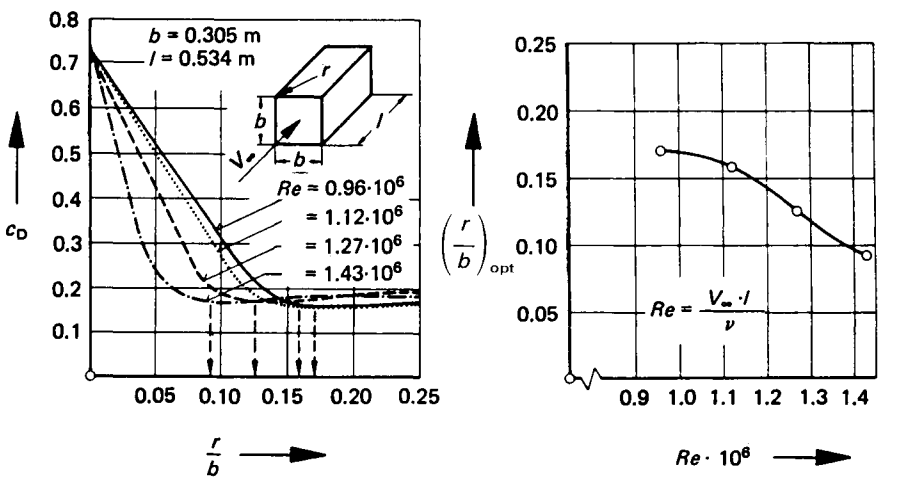

Figure 11.26 Influence of Reynolds number on the 'optimum' front end radius of a cuboid, after ref. 11.39

obviously traceable to the Reynolds number effect. It is known that the separation of the turbulent boundary layer is influenced by the Reynolds number; with increasing Reynolds number the location of the separation on a given body moves downstream. With larger Reynolds number the turbulent boundary layer can sustain greater adverse pressure gradients than with a small Reynolds number. This means that when the Reynolds number is large the air can flow around sharper bends without separation.

The measurements performed by Pawlowski,[11.39] which are reproduced in his original version in Fig. 1.38 and which are replotted in non-dimensional form in Fig. 11.26, confirm this. Further details on the influence of Reynolds number on optimum radii have been published by Cooper.[11.64] Similar Reynolds number effects have also been observed on other vehicle details. They are, as has been discussed in section 11.4.2, significant for wheels. Quantitative results—and only these count in the development of a vehicle—can therefore only be expected with the correct Reynolds number.

There are two ways to achieve the Reynolds number of the large version with scale models. Frequently the suggestion is made to increase the model scale but this would require a larger model wind tunnel. The advantage of the easy-to-handle model and the ease of quickly modifying the shape are rapidly lost with increasing dimensions. Limits therefore exist in this direction. In practice the largest model scale used for passenger vehicles is the 3/8 scale.

On the other hand, a frequent suggestion is to increase the air stream velocity in the model wind tunnels. Figure 11.27 (after ref. 11.38) shows that there is little scope for this either. Due to the bluntness of the vehicle body, greatly increased velocities are reached at individual points of the vehicle contour. As calculations and measurements on elliptical bodies of revolution and cylinders show, the critical Mach number, i.e. the Mach number for undisturbed oncoming flow, at which the speed of sound is first

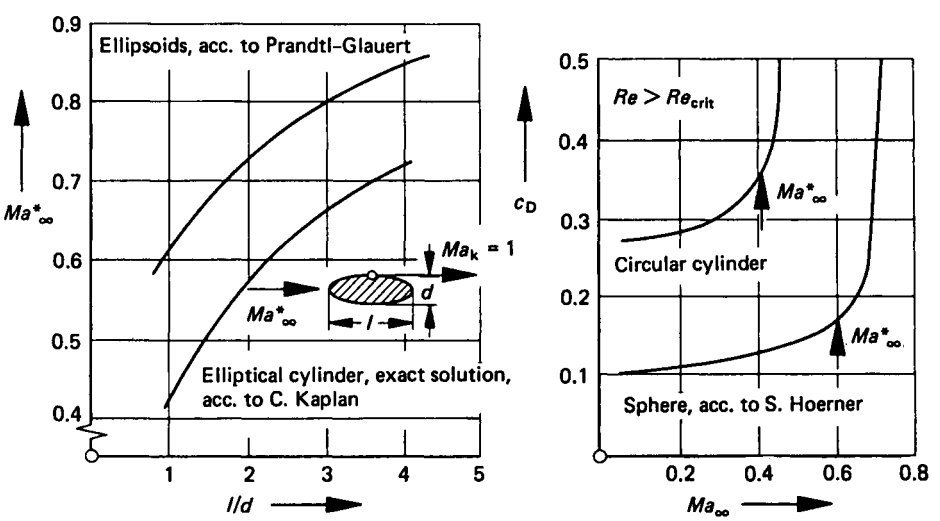

Figure 11.27 Critical Mach number and drag for bodies whose bluntness is comparable to that of passenger cars, after ref. 11.38

reached locally at the contour of the body, is reduced to very low values with increasing bluntness. Even below the critical Mach number the drag begins to increase due to compressibility effects. For vehicle shapes, this is probably much more difficult to calculate than the influence of the Reynolds number upon the local separation.

In wind tunnel tests on aircraft models a higher Reynolds number is sometimes simulated by artificially increasing the turbulence level of the wind tunnel air stream. In this manner, flow separation on a wing can be displaced to higher angles of attack, an effect that also occurs with increasing Reynolds number. This may possibly offer a solution. However, for the time being, quantitative information such as how great the turbulence level of the wind tunnel must be to simulate a certain Reynolds number, is not available. Artificial generation of turbulence also presents difficulties, because once produced, the turbulence decays along the flow. This procedure can therefore not yet be recommended for application in motor vehicle aerodynamics.

11.5 Existing automobile wind tunnels

11.5.1 Synopsis

The wind tunnels, climatic tunnels and climatic wind chambers used in industry and research centres for automobile aerodynamics are listed in Table 11.1. The tunnels are arranged according to the cross-section of the nozzle, without regard to the type of test section boundaries.

Wind tunnels with a nozzle cross-section of over $30\,m^2$ can be used for passenger car aerodynamics without limitations. Even small vans can be tested at full scale. For large commercial vehicles a scale of 1:2.5 is recommended. With low blockage, the Reynolds numbers for the full-scale version can still be achieved.

Tunnels with a nozzle cross-section between 15 and $25\,m^2$ are unnecessarily large for climatic engineering for passenger cars and small vans. For aerodynamic testing on vehicles at full scale they are suitable with limitations. Tunnels of this size can be improved with slotted or streamlined test section boundaries.

For *climatic tunnels*, a nozzle cross-section between 10 and $12\,m^2$ is sufficient. The prerequisite is that an empirical blockage correction factor be determined through calibration measurements in a large wind tunnel or on the road, which is then taken into consideration for the adjustment of the oncoming flow velocity. In part, an attempt is made to trim the air flow with the aid of baffles so that the pressure distribution on the vehicle corresponds as precisely as possible to that on the road. This would lead ultimately to a streamlined test section boundary, which, however, has not been practically applied to date.

Climatic wind chambers with a nozzle cross-section of $5\,m^2$ and smaller are suitable for climatic testing only with limitations, but can be used without limitations for cooling system development. The smaller the nozzle cross-section, the greater the effort that must be expended for calibration and flow guidance (baffles) for each new vehicle shape.

Table 11.1 Wind tunnels, climatic tunnels and climatic wind chambers in automobile aerodynamics

	A_T (m^2)	L_M (m)	V_{max} (km/h)	*TS*	*K*	*L* (m)	*P* (kW)	*Reference*
DNW	90.25	15.0	220	c	4.8	320	12700	11.66
	48.0	16.0	400	c	9.0			
General Motors	65.9	23	240	c	5	303	2950	11.21
Volkswagen	37.5	10.00	180	o	4.0	114.0	2600	11.41
Lockheed-Georgia	35.1	13.10	406	c	7.02	238.0	6700	11.51
MIRA	35.0	15.24	133	c	1.45	50.5	970	11.52
Daimler-Benz	32.6	10.00	270	o	3.53	125.0	4000	11.40
Fiat	30.0	10.50	200	o	4.0	144.0	1865	11.27
Volvo	27.06	15.8	200	sw	6.0	165.3	2300	11.71
Ford (Cologne)	24.0/8.6	10.0	182/298	o	4.0	124.0	1650/1960	11.62
Mazda	24	12.0	230	c/o	6	?	1600	11.63
Mitsubishi	24	12.0	216	c/o	?	?	2350	11.63
Ford (Dearborn)	23.2	9.15	201	c	3.80	?	1865	11.53
FKFS	22.5	9.5	220	o	4.41	150	2550	11.67
Porsche	22.3	12.0	230	sw	6.06	149.9	2200	11.68
Nissan	21.0	10.00	119	c	2.86	?	?	11.25
BMW	20.0	12.5	160	sw	3.66	45	1676	11.61
Toyota	17.5	8.00	200	c	3.66	95.0	1500	11.54
Nippon Soken	17.5/12	12.5/8.5	120/200	c	3.66	104	1450	11.63
Inst. Aérotechnique St. Cyr	15.0	10.00	144	sw	5.0	39.2	516	11.12
Fiat (2 × Climate)	12.0	11.60	160	o	4.0	99.0	560	11.27
JARI	12.0	10.00	205	c	4.06	83.3	1200	11.55
Pininfarina	11.75	9.5	185	o	6.2	27.3	1080	11.42
Ford (Cologne Climate)	11.0	9.00	180	c	6.0	113.4	1120	11.56
Sofica	11.0/4.3	16.5/14.0	80/170	c	?	?	380	11.45
FKFS	6.0	15.8	200	o	4.16	84	1000	11.69
Volkswagen II	6.0	7.2/6.0	170/180	o	6.0	73.4	460	11.70
Chrysler	4.74	8.6	190	o	5.56	58.8	560	11.57
Volvo	4.32	8.6	190	o	6.60	93.2	500	11.58
Behr	5.24	14.00	120	o	6.0	48.0	147	11.60
Opel	4.30	-	120	c	?	?	460	11.59
Audi	1.5	11.0	95	o	4.3	21.0	60	
Porsche	1.5	7.5	168	o	5.0	30	160	11.68

A_T Nozzle cross-section
L_M Length of test section
V_{max} Maximum wind speed

TS Type of test section:
o = open
c = closed
sw = slotted walls

K Contraction ratio
L Length of tunnel axis

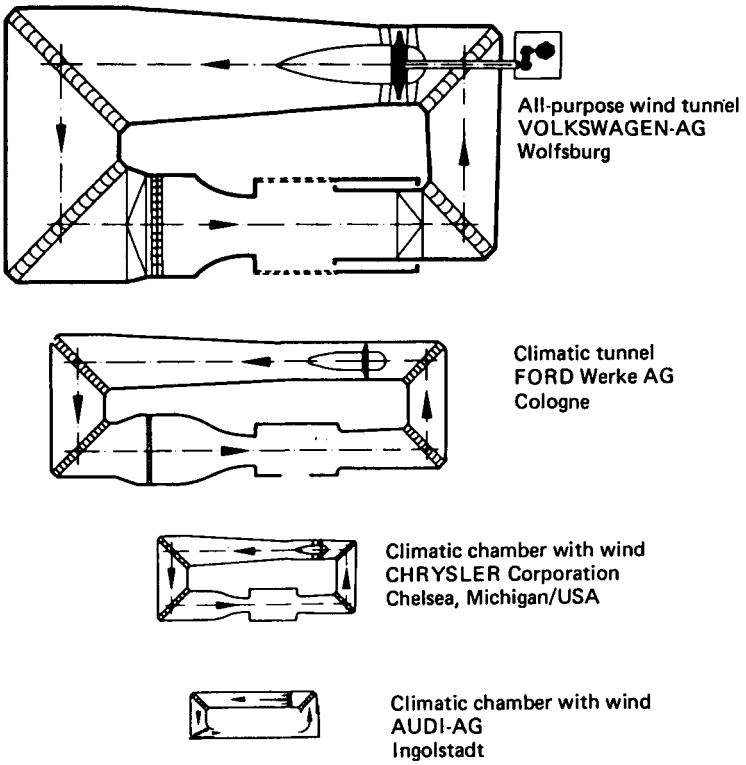

Figure 11.28 Size comparison between a large all-purpose wind tunnel, a climatic tunnel and two types of climatic chambers with wind

Figure 11.28 provides a pictorial comparison of the sizes of the various types of automobile wind tunnels. Figure 11.29 shows how the pressure distribution around the front of a car can approach reality even in a small climatic wind chamber by calibrating the wind velocity. Agreement of the pressure distribution in the area of the cooling air inlet is sufficient for cooling system development.

11.5.2 Large full-scale wind tunnels

Figure 11.30 shows the oldest full-scale automobile wind tunnel at Daimler-Benz AG in Stuttgart-Untertürkheim (see Kuhn[11.40]). This wind tunnel was designed under the direction of W. Kamm, opened in 1939 as part of the Forschungsinstitut für Kraftfahrwesen und Fahrzeugmotoren (FKFS), Stuttgart, Germany, and was completely overhauled in 1977, when it was taken over by Daimler-Benz AG. This wind tunnel is distinguished by an exceptionally high blowing velocity of V_{max} = 270 km/h. Such a high velocity is an advantage for the development of fast vehicles; it is then possible to examine directly the position of the vehicle resulting from the air forces and moments, and the effect of such changes upon the aerodynamics even at top speed.

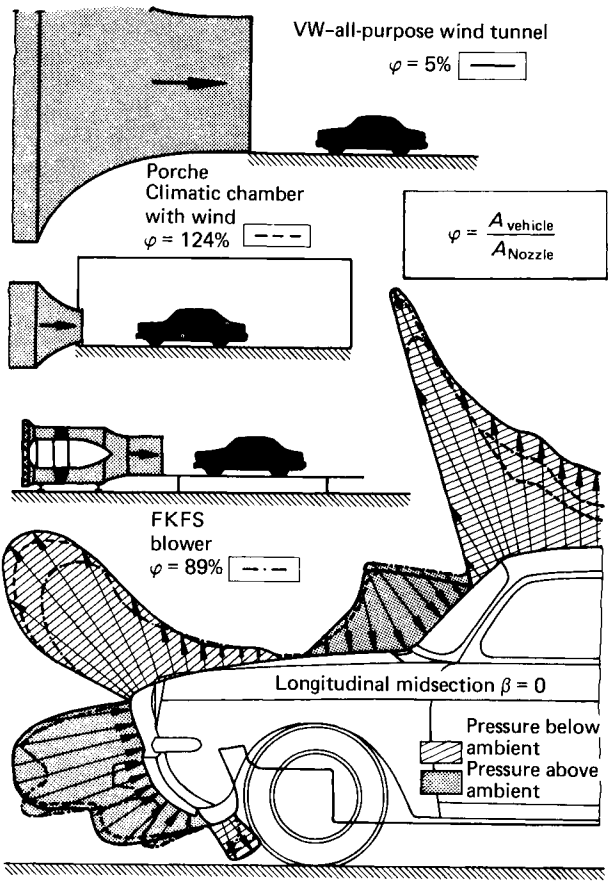

Figure 11.29 Comparison of the pressure distribution around the front of a car according to measurements in a large wind tunnel, a climatic chamber with wind and a blower, after R. Unger

For comparison, Fig. 11.31 shows the large climatic wind tunnel at Volkswagen AG in Wolfsburg, Germany. This tunnel (see Mörchen[11.41]) can be fully air conditioned; it is exceptionally well suited for all motor vehicle aerodynamic purposes. The limitation of the wind speed to V_{max} = 180 km/h is reasonable for a manufacturer of passenger cars and small vans, particularly as Reynolds number influences are unlikely and have never been observed for such high velocities.

The advantages and disadvantages of an all-purpose system, such as is represented by the Volkswagen AG climatic wind tunnel, in comparison to a 'wind tunnel centre', consisting of a large wind tunnel and climatic tunnels[11.27] are described in detail in ref. 11.7. For the time being, the Fiat concept of having separate tunnels for pure aerodynamic development work and for climatic tests can be said to be superior compared to the earlier approach of Volkswagen AG—having a general purpose climatic wind tunnel.

In any case, a large car manufacturer with a complete model line-up needs more than one aerodynamic test facility to do the large amount of

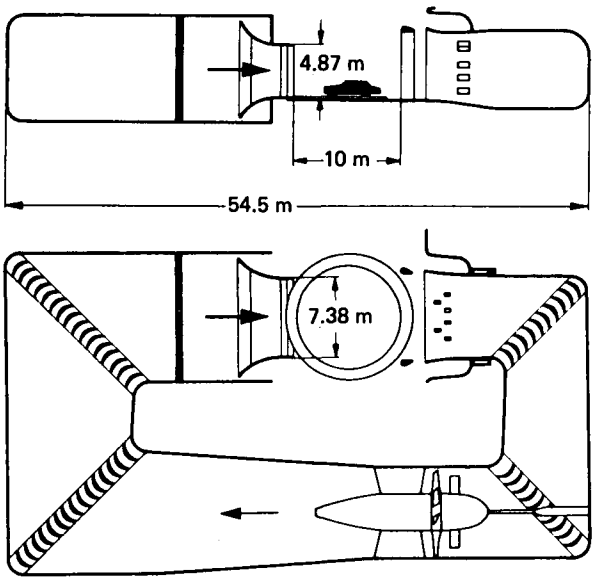

Nozzle cross-section: 32.6 m^2
Maximum wind speed: 270 km/h
Fan power: 4000 kW

Figure 11.30 Large full-scale wind tunnel of Daimler Benz AG, Stuttgart, Germany (earlier belonging to FKFS); after ref. 11.40

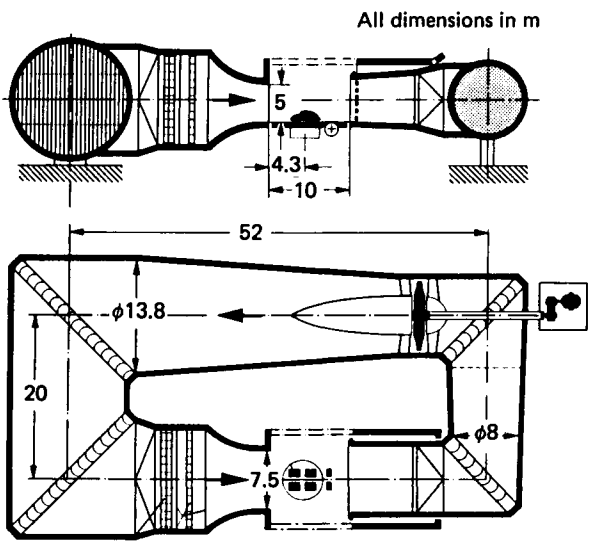

Nozzle cross-section: 37.5 m^2
Maximum wind speed: 175 km/h
Fan power: 2600 kW
Temperature range: –35°C to +40°C

Figure 11.31 Large full-scale climatic (all-purpose) wind tunnel of Volkswagen AG, Wolfsburg, Germany; after ref. 11.41

related development work. This implies specialized devices for aerodynamic and climatic tests. Each facility can be optimized to its purpose. Investment cost and operating cost are lower while flexibility is much higher.

11.5.3 Small full-scale wind tunnels

Small full-scale wind tunnels are those with test section cross-sections in the range 10 to 20 m^2. They either have open test sections or slotted walls. Blockage corrections have to be studied for each individual tunnel. Figure 11.32 shows the wind tunnel at Pininfarina, Turin, Italy, as an example of a small wind tunnel for testing full-size vehicles (see Morelli,[11.42] Cogotti[11.47]).

Nozzle cross-section: 11.75 m^2
Maximum wind speed: 185 km/h
Fan power: 1080 kW

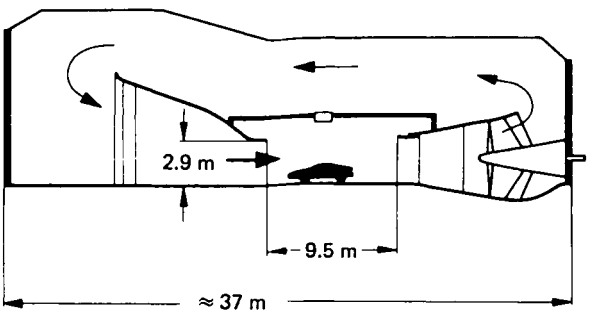

Figure 11.32 Small full-scale wind tunnel of Pininfarina, Turin, Italy; after ref. 11.42

This tunnel is a good example of the Eiffel type with air return in the test building, which is shaped to reduce the pressure loss in the return air path.

The aerodynamic development of models with a scale of 1:1 is subject to certain risks in such a small wind tunnel. The study of small changes, the basic idea of the detail optimization procedure, is only possible when the local flow fields are similar to those in the open air. The use of blockage corrections, which apply to overall forces and moments, is less certain. However, as will be discussed in section 11.5.7, a measurement comparison with large full-scale wind tunnels resulted in surprisingly favourable results for the Pininfarina wind tunnel.

11.5.4 Wind tunnels for scale models

Wind tunnels for scale models are not listed in Table 11.1; many such tunnels are occasionally used for vehicle aerodynamics. The MIRA model wind tunnel shown in Fig. 11.33, see Carr,[11.43] is intended to demonstrate how little expenditure is required for such a testing unit.

Smoke tunnels have been developed especially for flow observations on vehicles and their components. Isuzu Motors operates a 1 m^2 smoke tunnel, which allows three-dimensional phenomena to be made visible; Oda and Hoshino[11.44] have reported on this. Nissan has a smoke tunnel,

Nozzle cross-section: 2.12 m^2
Maximum wind speed: 160 km/h
Fan power: 37.3 kW.

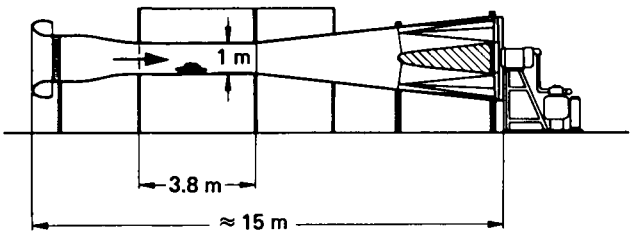

Figure 11.33 Quarter-scale model wind tunnel at MIRA, Nuneaton, UK; after ref. 11.43

which is used mostly for examination of details such as the cooling air duct on two-dimensional models.

11.5.5 Climatic tunnels

Figure 11.34 shows a typical climatic tunnel represented by that of Sofica, see Chenet.[11.45] An exchangeable nozzle allows the air stream cross-section to be adapted for testing passenger cars and small vans. Climatic tunnels of this type represent a very good, economical solution for the development of heaters and cooling systems. Climatic tunnels of this size are also operated by Fiat in Turin and by Ford in Cologne, see Table 11.1.

Nozzle cross-section: 11/4.3 m^2
Maximum wind speed: 80/170 km/h
Fan power: 280 kW
Temperature range: −50°C to +50°C

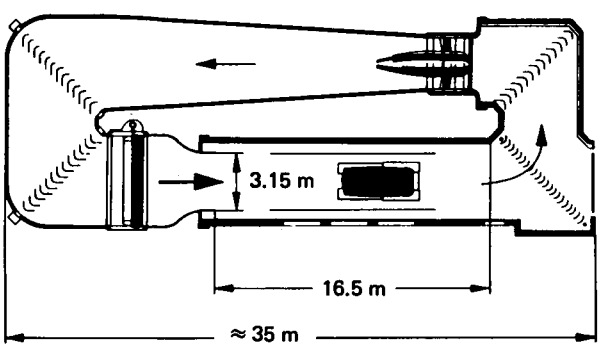

Figure 11.34 Climatic tunnel of Sofica, Paris, France; after ref. 11.45

11.5.6 Climatic wind chambers

In the construction of the climatic wind chamber shown in Fig. 11.35, the objective was to install the unit in a narrow room and simultaneously to allow easy access for the vehicle. Engine cooling tests performed in this chamber showed good agreement with tests performed in the climatic wind

Nozzle cross-section: 1.5 m^2
Maximum wind speed: 100 km/h
Fan power: 60 kW
Temperature range: −40°C bis +60°C

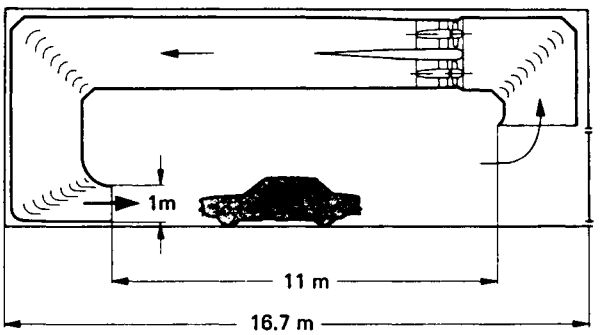

Figure 11.35 Climatic chamber with wind, Audi AG, Ingolstadt, Germany

tunnel at Volkswagen AG. This chamber is also used successfully for heater development by adjusting the test section boundaries with baffles. Climatic wind chambers of the size shown in Fig. 11.35, but with various different designs, are used in many places all over the world—mainly for cooling system development.

11.6 Comparative measurements between European and North American automobile wind tunnels

In order to assure the comparability of test data from different wind tunnels, an intensive correlation test programme has been performed between automotive wind tunnels in Europe, the US and Canada. The programme was started in Europe and results have been reported in detail by Buchheim et al.,[11.46] Cogotti et al.,[11.47] Costelli et al.,[11.48] and Carr.[11.49] It was later extended to the North American wind tunnels, see ref. 11.50. The same car, a Volkswagen 1600 notchback (Type 31) (see Fig. 4.17) was tested in the following wind tunnels (see Table 11.1) with open test section: Volkswagen AG (VW), Daimler-Benz (DB), Fiat (CRF), all large full-scale tunnels in the sense of section 11.5.2, and Pininfarina (PF), a small full-scale tunnel; with closed test section, the tunnels of Motor Industry Research Association (MIRA), Lockheed-Georgia, National Research Council Canada (NRC), General Motors (GM-ESAL), German-Dutch Wind Tunnel (DNW), all large full-scale tunnels; and, finally, the tunnel of the Institute Aérotechnique de St. Cyr (IAT), a small full-scale tunnel with slotted side walls. Details from the wind tunnels, the test procedure, the model and the corrections applied are to be found in refs 11.46 to 11.50. The results for the drag measurements are summarized in Fig. 11.36.

The measured drag coefficients are in a narrow band with a standard deviation of ±2.2 per cent, corresponding to $\Delta\bar{c}_D = \pm 0.009$. In view of the large technical differences among the wind tunnels considered this may be called a good agreement in drag data. On the other hand, the largest

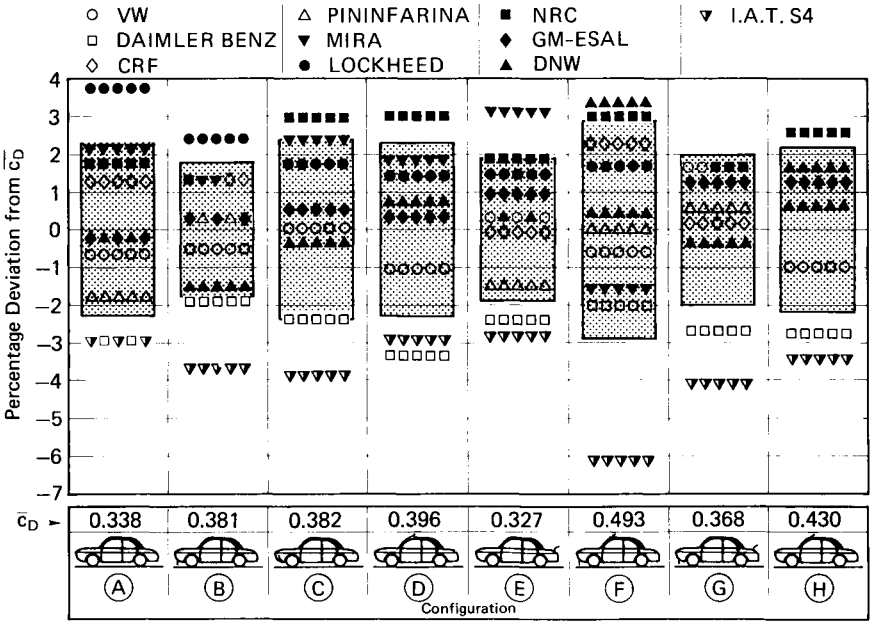

$\overline{c_D}$ = Drag coefficient mean of 10(8) wind tunnels
Standard deviation from mean of 10(8) wind tunnels

Figure 11.36 Comparison of drag measurements in major European and North American automobile wind tunnels, after ref. 11.50

spread of data, which was 9.3 per cent on configuration F, shows that occasionally significant differences may occur.

The data show some systematic differences: St. Cyr and Daimler-Benz data are always below mean value (not that the mean is necessarily the true value). Lockheed and NRC data are above the mean; DNW, GM-ESAL, VW and CRF are close to the mean. Despite the applied corrections the drag figures from the tunnels with closed test section are generally higher than those from open test sections (for which no corrections at all are applied). Surprisingly, the data of the smallest tunnel, the Pininfarina, are well within the standard deviation of the large tunnels.

A more systematic way to look at comparative data is to compare drag changes due to minor or greater modifications of individual body details, see Fig. 11.37, after Buchheim et al.[11.50] For example, the drag reduction due to a rear spoiler was 1.3 per cent in one tunnel and 5.1 per cent in another. The first figure may well be considered not to justify the expense of a rear spoiler, while the latter may suggest the opposite. No explanations have been offered to explain these discrepancies. Furthermore, Buchheim et al.[11.50] emphasize that comparing data from cars other than the tested one—e.g. fastbacks and squarebacks with their related rear flow characteristics—may lead to somewhat different results, see Cogotti et al.[11.47] and Costelli et al.[11.48]

As reported by Buchheim et al. in ref. 11.50, the agreement between the lift figures obtained in the tunnels is not as good. Whether the measured differences result from the different flow patterns (angle of attack of the air

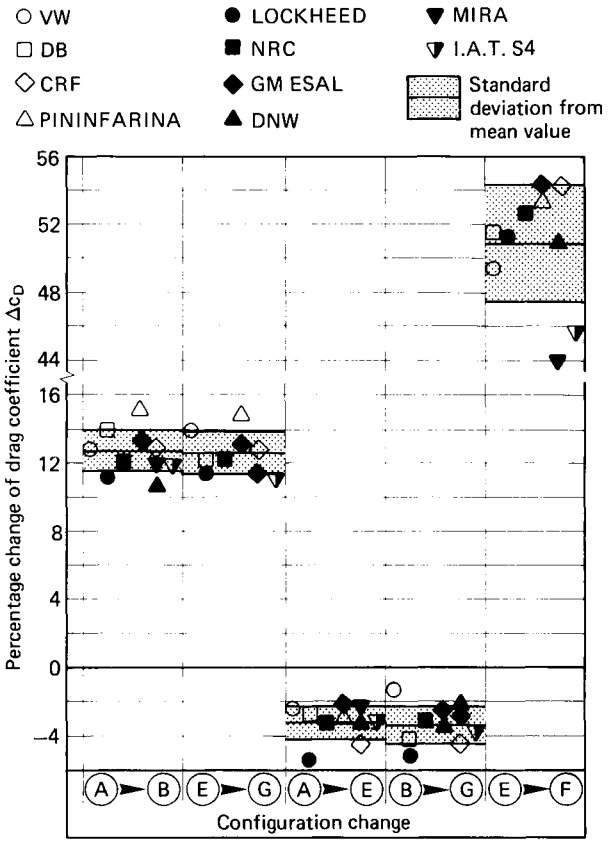

Figure 11.37 Change of drag subsequent to shape modifications, comparison between wind tunnels; after ref. 11.50

stream) in the individual wind tunnels or from the measurement techniques (consideration of the lift on the wheel support plates of the balance), has yet to be clarified.

In the Fiat tunnel, which has a floor boundary layer suction device, comparative measurements were performed with and without floor boundary layer suction. These confirmed the findings of Hucho, Janssen and Schwarz[11.22] and model tests performed by Carr and Hassell:[11.30] suction of the floor boundary layer has no measurable influence upon the aerodynamic drag of passenger cars.

11.7 Final comments and prospects

The large number of testing facilities for research and development in the area of automobile aerodynamics indicates the high priority placed on this area of specialization by motor vehicle engineering. Of particular note is the multiplicity of types and sizes of such facilities. In spite of the nearly identical objectives, the various vehicle manufacturers have arrived at solutions which differ considerably from one another. This is in part

attributable to the fact that particular objectives in the field of automobile aerodynamics are not given the same significance by all, and in part to the fact that, over time, the objectives have changed.

The rapidly increasing significance of fuel economy is bringing the aerodynamic drag of vehicles more and more to the fore. This makes it all the more important to be able to measure this figure reliably in a wind tunnel.

Reliable wind tunnel corrections must be derived from the results of comparative measurements—both existing and those still outstanding. Inclusion of further wind tunnels will make it possible to confirm these correction factors on a wider basis.

It is known that the individual users of one large wind tunnel in the US use different, company-specific wind tunnel correction factors for the test data obtained in this tunnel. The result is that various c_D values are derived from one set of uncorrected test data, depending upon the user. By computing and agreeing upon standardized wind tunnel correction factors, this situation, which makes it difficult for the arguments of automotive aerodynamic engineers to be taken seriously, must be surmounted.

11.8 Notation

A	frontal area of the vehicle
A_S	cross-sectional area of settling chamber
A_T	cross-sectional area of wind tunnel air stream
D	drag, Figs 11.2 and 11.3
K	contraction ratio, Fig. 11.9
K_{new}, K_o	contraction ratio, Fig. 11.10
L	lift, Figs 11.2 and 11.3
L_K	length of test section
M	pitching moment, Figs 11.2 and 11.3
Ma	Mach number, Fig. 11.27
P	drive power of wind tunnel
P_{new}, P_o	drive power of wind tunnel, Fig. 11.10
$\dot{Q}_c$	heat flux
Q	suction volume flow
Re	Reynolds number, Eqn 2.4
Tu	turbulence level
U	flow velocity
V	vehicle speed
V	wind velocity
V_∞	oncoming flow velocity
V_B	belt speed
c_D	drag coefficient, Eqn 1.2
c_p	pressure coefficient, Eqn 2.8
c^*_Q	suction parameter
d	diameter, Fig. 11.9
e	ground clearance, Fig. 4.111
h	height above ground
l	vehicle length

p	static pressure
p_∞	static pressure in undisturbed flow (free stream)
r	contour radius
s	width of suction slot, Fig. 11.14
u'	turbulent velocity variation
v_s	velocity in suction slot, Fig. 11.14
w	vehicle width
x, y, z	orthogonal coordinate system
α	angle of attack, Fig. 11.1
β	angle of yaw, Fig. 11.1
δ	boundary layer thickness
δ_1	displacement thickness of boundary layer
ν	kinematic viscosity of the air
ρ	air density
φ	blockage ratio, Fig. 11.29
ω	angular velocity of the wheel